Development 140, 2245 (2013) doi:10.1242/dev.096974

Ptk7 promotes non-canonical Wnt/PCP-mediated morphogenesis and inhibits Wnt/β-catenin-dependent cell fate decisions during vertebrate development

Madeline Hayes, Mizue Naito, Avais Daulat, Stephane Angers and Brian Ciruna

There was an error published in *Development* **140**, 1807-1818.

On p. 1813, the title of Fig. 5 should read: *Ptk7* overexpression potentiates exogenous non-canonical Wnt/PCP activity.

The authors apologise to readers for this mistake.

Development 140, 1807-1818 (2013) doi:10.1242/dev.090183

Ptk7 promotes non-canonical Wnt/PCP-mediated morphogenesis and inhibits Wnt/β-catenin-dependent cell fate decisions during vertebrate development

Madeline Hayes[1,2], Mizue Naito[1,*], Avais Daulat[3,‡], Stephane Angers[3] and Brian Ciruna[1,2,§]

SUMMARY

Using zebrafish, we have characterised the function of Protein tyrosine kinase 7 (Ptk7), a transmembrane pseudokinase implicated in Wnt signal transduction during embryonic development and in cancer. Ptk7 is a known regulator of mammalian neural tube closure and *Xenopus* convergent extension movement. However, conflicting reports have indicated both positive and negative roles for Ptk7 in canonical Wnt/β-catenin signalling. To clarify the function of Ptk7 in vertebrate embryonic patterning and morphogenesis, we generated maternal-zygotic (MZ) *ptk7* mutant zebrafish using a zinc-finger nuclease (ZFN) gene targeting approach. Early loss of zebrafish Ptk7 leads to defects in axial convergence and extension, neural tube morphogenesis and loss of planar cell polarity (PCP). Furthermore, during late gastrula and segmentation stages, we observe significant upregulation of β-catenin target gene expression and demonstrate a clear role for Ptk7 in attenuating canonical Wnt/β-catenin activity *in vivo*. MZ*ptk7* mutants display expanded differentiation of paraxial mesoderm within the tailbud, suggesting an important role for Ptk7 in regulating canonical Wnt-dependent fate specification within posterior stem cell pools post-gastrulation. Furthermore, we demonstrate that a plasma membrane-tethered Ptk7 extracellular fragment is sufficient to rescue both PCP morphogenesis and Wnt/β-catenin patterning defects in MZ*ptk7* mutant embryos. Our results indicate that the extracellular domain of Ptk7 acts as an important regulator of both non-canonical Wnt/PCP and canonical Wnt/β-catenin signalling in multiple vertebrate developmental contexts, with important implications for the upregulated *PTK7* expression observed in human cancers.

KEY WORDS: Ptk7, Cancer, Morphogenesis, Planar cell polarity, Stem cell fate, Wnt signal transduction, Zebrafish

INTRODUCTION

Wnt signalling controls a diverse range of developmental processes from tissue specification to axial morphogenesis (Moon et al., 1997; Wodarz and Nusse, 1998). Pathway activation is carefully controlled, and misregulated Wnt activity has been implicated in a variety of developmental abnormalities (Ikeya et al., 1997; Yamaguchi et al., 1999a; Hamblet et al., 2002; Wallingford and Harland, 2002). Wnt signalling is also required for stem cell maintenance and adult tissue homeostasis, with perturbations frequently implicated in cancer formation (Logan and Nusse, 2004; Polakis, 2007).

Wnt signal transduction pathways are highly conserved among metazoans. In the canonical Wnt/β-catenin pathway, Wnt ligands bind Frizzled (Fz) receptor/low density lipoprotein receptor-related protein (LRP) complexes at the cell surface. Wnt signals, transduced through Dishevelled (Dvl), inhibit GSK-3β-APC-Axin complex-directed proteosomal degradation of β-catenin. Nuclear translocation of stable β-catenin leads to the transcriptional activation of genes involved in cell replication, growth, apoptosis and self-renewal. During embryogenesis, canonical Wnt/β-catenin signalling also controls diverse cell fate determination events, including dorsal-ventral patterning (De Robertis et al., 2000; De Robertis and Kuroda, 2004; Schier and Talbot, 2005), cardiac and central nervous system differentiation (Yamaguchi et al., 1999b; Ryu et al., 2001), and the specification of paraxial mesoderm cell fate from a bi-potential neural/mesodermal progenitor cell pool within the vertebrate tailbud (Martin and Kimelman, 2012; Nowotschin et al., 2012).

Multiple β-catenin-independent pathways can also be activated upon Wnt binding to Fz receptors (Kohn and Moon, 2005; Jenny and Mlodzik, 2006), the best characterised of which is the planar cell polarity (PCP) pathway. PCP coordinates the uniform orientation of cell structure and cell movement within the plane of a tissue (Zallen, 2007). In vertebrates, this is required to drive convergence and extension (C&E) – polarised cell movements that narrow and extend the body axis (Keller, 2002; Wallingford and Harland, 2002; Yin et al., 2009). Mutation of vertebrate PCP genes block these cell movements, resulting in broader and shorter tissues, and neural tube closure defects (Simons and Mlodzik, 2008; Yin et al., 2009).

A core 'cassette' of proteins establish PCP across animal species. As in Wnt/β-catenin signalling, PCP requires Fz activation and subsequent membrane localisation of Dvl. In vertebrates, Fz activation is thought to occur through binding of Wnt5 and Wnt11 ligands (Yin et al., 2009). Other proteins, specific to PCP, regulate Fz-Dvl activity. They include the transmembrane protein Van Gogh (Vang) and the cytosolic effector protein Prickle (Pk) (Jenny et al., 2003). Asymmetric subcellular localisation of PCP molecules is key to cell polarity, creating regionalised activation of Rho kinase, and local reorganisation of the actin cytoskeleton (Strutt and Strutt, 2009).

Differential activation of alternative Wnt pathways is not entirely ligand dependent; in some contexts, Wnt5a can activate Wnt/β-

[1]Program in Developmental & Stem Cell Biology, The Hospital for Sick Children, Toronto, ON, M5G 1X8, Canada. [2]Department of Molecular Genetics, The University of Toronto, ON, M5S 1A8, Canada. [3]Departments of Biochemistry and Pharmaceutical Sciences, The University of Toronto, ON, M5S 1A8, Canada.

*Present address: Department of Microbiology, Cornell University, Ithaca, NY 14853-8101, USA
‡Present address: Inserm, U891, Centre de Recherche en Cancérologie de Marseille, France
§Author for correspondence (ciruna@sickkids.ca)

Accepted 19 February 2013

catenin signalling (Clevers, 2006). Rather, the cellular complement of Fz co-receptors dictates Wnt pathway choice (van Amerongen et al., 2008). Lrp6 activates canonical Wnt/β-catenin responses (Tamai et al., 2000), whereas the ROR transmembrane kinases can specifically bind Wnt5a and inhibit Wnt/β-catenin signalling (Mikels and Nusse, 2006). Ror2 can also form a Wnt-induced complex with the PCP regulator Van Gogh-like 2 (Vangl2) to affect tissue polarity (Gao et al., 2011). Furthermore, regulatory proteins can shift the balance between alternative Wnt pathway activation. The metastasis-associated transmembrane protein Wnt-activated inhibitory factor 1 (Waif1), for example, inhibits Wnt/β-catenin signalling and activates non-canonical Wnt pathways by modifying Lrp6 subcellular localisation (Kagermeier-Schenk et al., 2011).

Protein tyrosine kinase 7 (Ptk7; also known as colon carcinoma kinase-4, CCK4) is an atypical receptor tyrosine kinase that has also been implicated in vertebrate Wnt signal transduction (Lu et al., 2004; Shnitsar and Borchers, 2008; Paudyal et al., 2010; Peradziryi et al., 2011; Puppo et al., 2011). Initially identified in metastatic colon cancer, *PTK7* expression is also upregulated in acute myeloid leukaemia (AML) and multiple other cancer types (Mossie et al., 1995; Easty et al., 1997; Endoh et al., 2004; Müller-Tidow et al., 2004; Gorringe et al., 2005; Gobble et al., 2011). Full-length Ptk7 contains seven extracellular immunoglobulin (Ig)-like domains, a transmembrane domain and a catalytically inactive kinase domain; the Ptk7 ATP-binding motif is mutated (Mossie et al., 1995) and tyrosine phosphorylation (activation) is not observed following overexpression in COS-1 or HEK293 cells, or in *in vitro* kinase assays (Mossie et al., 1995; Jung et al., 2004). Orthologues have been identified in mouse, *Xenopus*, chick (KLG), *Drosophila* (Off-track, OTK) and Hydra (Lemon), and have been implicated in various morphogenetic processes in each system (Chou and Hayman, 1991; Lee et al., 1993; Mossie et al., 1995; Miller and Steele, 2000; Winberg et al., 2001; Jung et al., 2004). Mouse *Ptk7* mutant embryos die perinatally and display shorter and wider body axes, loss of mesodermal cell polarity, and neural tube closure defects, abnormalities attributed to defective PCP (Lu et al., 2004; Yen et al., 2009; Paudyal et al., 2010). Similar phenotypes are observed upon morpholino (MO) knockdown of *PTK7* in *Xenopus* (Lu et al., 2004).

There is also evidence that Ptk7 might regulate canonical Wnt/β-catenin signalling. Ptk7 co-immunoprecipitates (co-IPs) with Wnt3a and Wnt8 (Peradziryi et al., 2011), requiring a Ptk7 and Fz7 receptor complex that has been demonstrated to be both dependent (Shnitsar and Borchers, 2008) and independent (Peradziryi et al., 2011) of interactions with Dvl. The Ptk7 pseudokinase domain can also interact with β-catenin in yeast-two-hybrid assays, and mammalian cell co-IPs. Moreover, overexpression of *PTK7ΔICD* constructs, which lack the intracellular pseudokinase domain, suppresses Wnt/β-catenin dorsal organiser gene expression in *Xenopus* (Puppo et al., 2011).

Functional investigations into the role for Ptk7 in vertebrate Wnt/β-catenin signalling remain inconclusive. Wnt/β-catenin patterning defects have not been reported in three independent analyses of *Ptk7* mutant mice (Lu et al., 2004; Yen et al., 2009; Paudyal et al., 2010). In *Xenopus*, MO knockdown of *PTK7* suppresses Wnt/β-catenin Spemann organiser formation and *siamois* promoter activation (Puppo et al., 2011), suggesting that Ptk7 potentiates canonical Wnt signalling. However, MO knockdown of *PTK7* in *Xenopus* animal cap explants enhances the ability of exogenous Wnt8 to activate β-catenin signalling (Peradziryi et al., 2011), suggesting that Ptk7 inhibits the Wnt/β-catenin pathway.

In order to clarify the function of Ptk7 in vertebrate embryonic patterning and morphogenesis, we cloned the single zebrafish *ptk7* orthologue and generated a loss-of-function allele. Through analysis of maternal-zygotic (MZ) *ptk7* mutant embryos, we demonstrate a requirement for Ptk7 in potentiating PCP-dependent morphogenesis, and establish a clear role for Ptk7 in attenuating canonical Wnt/β-catenin signalling *in vivo*. Finally, we demonstrate that the highly conserved pseudokinase domain is not required for Ptk7 activity in axial morphogenesis and mesodermal cell fate determination. Rather, a plasma membrane-tethered Ptk7 extracellular domain fragment is sufficient to rescue these PCP and canonical Wnt-dependent activities in MZ*ptk7* mutant embryos.

MATERIALS AND METHODS

Zebrafish strains

Wild-type and mutant zebrafish strains were raised under standard conditions (Westerfield, 2007). The *vangl2* mutant allele *tri(tk50f)* contains a deletion in the *vangl2* coding sequence (Jessen et al., 2002).

Generation of *ptk7* mutant

ZiFiT software (http://zifit.partners.org/ZiFiT/) was used to identify potential target sites in *ptk7*. Using the Oligomerized Pool Engineering (OPEN) system (Maeder et al., 2008; Foley et al., 2009) method, two selections (one for each half-site) were made. A bacterial one-hybrid assay was used to test specificity of the engineered arrays against a sequence-specific pH3U3 reporter vector expressed in USO*ΔhisΔpyrΔrpoZ* cells (Meng et al., 2008). The zinc-finger cassette was inserted into pCS2+ expression vectors. The sequences for left and right zinc-fingers are listed in supplementary material Table S1.

mRNA (80 pg) for each ZFN was injected into one-cell-stage embryos (F0). F1 genomic DNA was screened for mutations in *ptk7* using a PCR-based assay: forward, 5′-CGAAGGCCGCTGAGGATGA-3′; reverse, 5′-CAGAAAACGCATGAAGTGACCAGC-3′. *Sfa*N1 endonuclease (NEB) was used to identify potential mutations.

Plasmids and embryo microinjections

Ptk7 was amplified from 24 hours post-fertilisation (hpf) wild-type cDNA made using oligo(dT)$_{12-18}$ primer (Invitrogen) and SuperscriptII (Invitrogen) as per manufacturer's instructions. *Ptk7* was cloned into pCS2+ using Gateway technology (Invitrogen). *Ptk7ΔICD*, *ptk7 egfrTM*, *ptk7ΔECD* and *ptk7 ECD* were amplified from full-length *ptk7* (supplementary material Table S2). The mMESSAGE mMACHINE System (Ambion) was used to make mRNA. All injections were performed at the one-cell stage.

Whole-mount *in situ* hybridization (WISH)

Antisense RNA probes were prepared by *in vitro* transcription (DIG RNA Labeling Kit, Roche) in the presence of digoxigenin-11-UTP from linearized DNA templates. Embryos were cleared in 100% methanol, mounted in benzylbenzoate:benzylalcohol (2:1), and imaged on an Axio Imager.M1 (Zeiss) compound microscope.

Quantitative reverse-transcriptase PCR (qRT-PCR)

Total RNA was extracted using TRIzol reagent (Invitrogen) according to manufacturer's recommendations. First-strand cDNA was made using SuperScript II reverse transcriptase (Invitrogen) and oligo(dT)$_{12-18}$ primer (Invitrogen). For primer sequences, see supplementary material Table S2. SYBR green (Applied Biosystems) was used according to manufacturer's recommendations. All analyses were carried out in triplicate using a Light Cycler 480 (Roche) platform. Fifty amplification cycles were performed, with each cycle consisting of 95°C for 10 seconds, 60°C for 20 seconds and 72°C for 30 seconds. Amplification and dissociation curves generated by the Light Cycler 480 Software release 1.5.0 SP4 were used for gene expression analysis. Ct values were obtained for each gene and normalised to *Gapdh*. Fold change was calculated relative to wild-type expression according to the equation: $2^{-\Delta\Delta Ct}$. Standard error was calculated as standard deviation of the fold change according to the equation: $stdev_{foldchange}=(ln2)(stdev_{\Delta\Delta Ct})(2^{-\Delta\Delta Ct})$, where $stdev_{\Delta\Delta Ct}=\sqrt{(stdev\ of\ reference)^2 + (stdev\ of\ gene\ of\ interest)^2}$. All graphs are representative of

two independent experiments with three technical replicates each. Statistical significance was calculated using Student's *t*-test.

Confocal imaging

Live embryos were immobilised on a coverslip in 0.8% agarose, and imaged using a Zeiss LSM 710 microscope. *z*-stacks were collected and processed using ImageJ software.

TopFlash assay

TopFlash was conducted in human HEK293T cells as previously described (Angers et al., 2006; Lui et al., 2011). Lentiviruses containing the superTopFlash β-catenin-dependent luciferase reporter (Firefly luciferase) and pRL-TK (*Renilla* luciferase) were produced and used to establish stable HEK293T Wnt-reporter lines. Cells were seeded on 24-well plates, followed by cDNA transfection with polyethylenimine (PEI). Media was replaced with a 1:1 mix of fresh DMEM:Wnt3A or DMEM:Control conditioned media. Cells were assayed 16 hours after stimulation, performed in accordance with the Dual Luciferase assay specifications (Promega) using an Envision 2103 Multilabel Plate Reader (PerkinElmer).

RESULTS

ptk7 sequence and expression is well conserved among vertebrates

Full-length zebrafish *ptk7* coding sequence was cloned from a 24 hpf cDNA library using primers designed against predicted open reading frame sequence (supplementary material Fig. S1). Zebrafish Ptk7 protein contains 1061 amino acids and consists of an extracellular domain with seven immunoglobulin-like loops, a single transmembrane domain and an intracellular domain with structural features typical of a tyrosine kinase (van der Geer et al., 1994) (Fig. 1A). However, as with all vertebrate Ptk7 orthologues, the DFG triplet believed to be essential for catalytic activity is modified in zebrafish Ptk7 (supplementary material Fig. S1), classifying it as a pseudokinase. Overall, zebrafish Ptk7 is highly conserved with chicken (Chou and Hayman, 1991), *Xenopus* (Lu et al., 2004) human and mouse (Mossie et al., 1995; Jung et al., 2004) proteins, with greatest conservation observed within transmembrane and intracellular pseudokinase domains (Fig. 1A). We were unable to find evidence of additional *ptk7* homologues in the zebrafish genome through nucleotide BLAST searches against the Zv9 assembly.

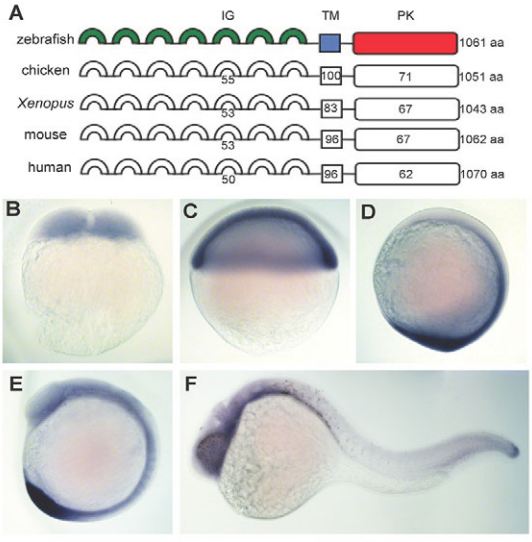

Fig. 1. Zebrafish Ptk7 structure and embryonic expression. (**A**) Domain structure of zebrafish Ptk7 and its homology to chicken (KLG), *Xenopus*, mouse and human orthologues. Numbers indicate percentage amino-acid identity within extracellular immunoglobulin (IG), transmembrane (TM) and intracellular pseudokinase (PK) domains. (**B-F**) WISH of *ptk7* expression throughout the first 24 hours of development. Lateral views of two-cell (0.75 hpf, B), shield (6 hpf; C), bud (10 hpf; D), 10- to 12-somite (15 hpf; E) and 24 hpf (F) stage embryos are shown.

Using whole-mount RNA *in situ* hybridisation (WISH), we observed *ptk7* expression at the two-cell stage, prior to mid-blastula transition (MBT) and initiation of zygotic transcription, indicating strong maternal contribution (Fig. 1B). *ptk7* expression is ubiquitous at the onset of gastrulation (shield stage; Fig. 1C), and is pronounced in axial, paraxial and tailbud lineages during late-gastrula stages (Fig. 1D). Post-gastrulation, *ptk7* is expressed in the head, neural tube and somites, with the highest level of expression observed in the tailbud (Fig. 1E). *ptk7* expression within the tailbud persists until 24 hpf (Fig. 1F). The expression of zebrafish *ptk7* is similar to that observed in *Xenopus* and mouse (Lu et al., 2004), encouraging us to examine Ptk7 function further using zebrafish as our model system.

Overexpression of *ptk7* disrupts embryonic patterning and morphogenesis

As a first investigation into Ptk7 function, we injected high levels of *ptk7* mRNA into single-cell-stage embryos (within 10 minutes of fertilisation) and analysed its effect on embryonic patterning and morphogenesis. Consistent with published results, overexpression of *ptk7* caused phenotypes associated with abnormal PCP (Fig. 2B), including defects in axial extension as well as dorsal curvatures of the posterior tail (observed with *vangl2* overexpression) (Borovina et al., 2010). However, overexpression of *ptk7* also yielded dorsalised embryos (32%, *n*=100; Fig. 2C), a phenotype not associated with PCP signalling mutants.

Canonical Wnt/β-catenin signals strongly influence dorsal-ventral pattern, first promoting dorsal organiser formation prior to MBT and then opposing its maintenance during late-blastula stages (De Robertis et al., 2000; De Robertis and Kuroda, 2004; Schier and Talbot, 2005). At 4 hpf, we could not detect changes in expression of *bozozok* (*boz*; *dharma* – Zebrafish Information Network) and *chordin* (*chd*), direct targets of β-catenin at the dorsal organiser (Wylie et al., 1996; Fekany et al., 1999; Solnica-Krezel and Driever, 2001), in *ptk7*-injected embryos (supplementary material Fig. S2A). However, later shield-staged embryos displayed lateral expansion of *chd* (47%, *n*=30; Fig. 2D,E) as well as reduced expression of the ventral Wnt-target gene *vox* (Ramel and Lekven, 2004) (77%, *n*=30; Fig. 2F,G). Moreover, *ptk7* overexpression resulted in reduced expression of the β-catenin target *axin2*, as assayed by WISH (Fig. 2H,I) and qRT-PCR (supplementary material Fig. S2B). Our results suggest that *ptk7* overexpression may attenuate the ventralising activity of canonical Wnt signals during early embryogenesis.

Ptk7 inhibits exogenous Wnt/β-catenin signalling activity

To investigate further the role for zebrafish Ptk7 in canonical Wnt signalling, we examined the effects of *ptk7* overexpression on exogenous Wnt/β-catenin activity. In zebrafish embryos, ectopic expression of *wnt8* produces phenotypes characteristic of Wnt/β-catenin activation; namely, defects in dorsoventral patterning and posteriorisation of the neuroectoderm (Lekven et al., 2001) (Fig. 2J). Strikingly, co-injection of *ptk7* mRNA largely rescued the loss of forebrain and eye-field associated with *wnt8* overexpression (94%, 52/55; Fig. 2J), suggesting that Ptk7 can inhibit exogenous Wnt/β-catenin activity.

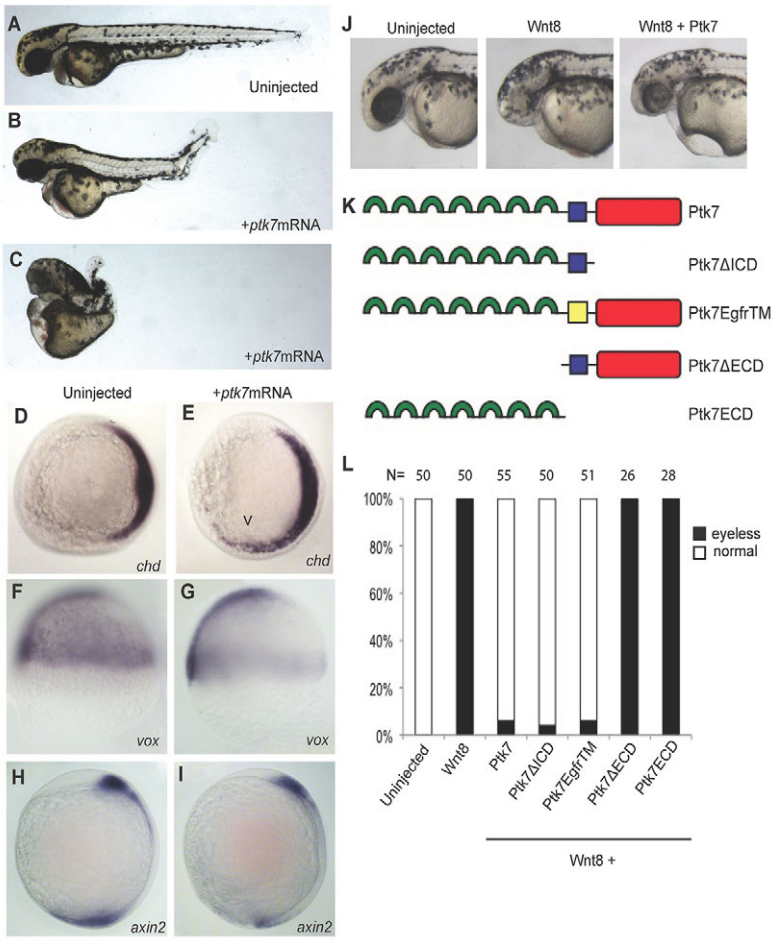

Fig. 2. *Ptk7* overexpression disrupts embryonic patterning and morphogenesis and inhibits exogenous Wnt/β-catenin activity. (**A**) Lateral view of uninjected control embryos at 36 hpf. (**B**,**C**) Embryos injected with *ptk7* (400 pg) mRNA at the one-cell stage exhibit axial morphogenesis (B) and dorsoventral patterning defects (C). (**D**,**E**) Whole-mount *in situ* hybridisation (WISH) demonstrating *chordin* (*chd*) expression in control (D) and *ptk7* (400 pg) mRNA-injected (E) embryos at shield stage (animal pole view, dorsal right). Arrowhead indicates lateral expansion of *chd* expression in embryos overexpressing Ptk7. (**F**,**G**) WISH of *vox* expression in control (F) and *ptk7* (400 pg) mRNA-injected (G) embryos at shield stage (lateral view, dorsal right). (**H**,**I**) WISH for *axin2* in control (H) and *ptk7* (400 pg) mRNA-injected (I) embryos at bud stage (lateral view). Reduced *vox* and a*xin2* expression is observed in embryos overexpressing Ptk7. (**J**) Overexpression of *wnt8* (10 pg) disrupts CNS pattern, as demonstrated by loss of eyes and reduced forebrain at 36 hpf. Co-injection of *ptk7* (300 pg) mRNA can largely rescue these *wnt8*-induced phenotypes. (**K**) Schematic of Ptk7 mutant isoforms generated for structure-function and rescue experiments. (**L**) Quantification of phenotypes observed upon injection of *wnt8* (10 pg) mRNA, and upon co-injection of *wnt8* with full length *ptk7* (300 pg), *ptk7ΔICD* (200 pg), *ptk7 egfrTM* (300 pg), *ptk7ΔECD* (150 pg) and *ptk7 ECD* (200 pg) mRNA. mRNA concentrations were adjusted to yield equimolar amounts of truncated/mutant Ptk7 protein. Embryos were scored as being 'eyeless' if the eye was either completely absent or <25% the size of uninjected controls.

To determine which domains of Ptk7 protein are required for this function, we tested the ability of deletion and substitution mutants (Fig. 2K) to rescue *wnt8* overexpression defects. An intracellular domain deletion construct (*ptk7ΔICD*) rescued *wnt8*-induced eye and forebrain defects to the same extent as full-length *ptk7* (96%, *n*=50; Fig. 2L), as did substitution of the Ptk7 transmembrane domain with that of Egfr (*ptk7EgfrTM*; 94%, *n*=51; Fig. 2L). Expression of an extracellular domain deletion mutant (*ptk7ΔECD*) failed to rescue *wnt8* overexpression (0/26; Fig. 2L), as did expression of a secreted extracellular domain (*ptk7ECD*) fragment (0/28; Fig. 2L). Our results indicate that the highly conserved Ptk7 pseudokinase and transmembrane domains are not required to inhibit Wnt/β-catenin activity. Rather, a membrane-tethered Ptk7 extracellular domain is crucial for this function.

Ptk7 expression similarly abrogated Wnt3a-stimulated TOP-Flash luciferase activity in HEK293T cells. Deletion of the intracellular domain (*ptk7ΔICD*) and substitution of the transmembrane domain (*ptk7EgfrTM*) did not impair protein function (supplementary material Fig. S3). However, *ptk7ΔECD* expression failed to inhibit Wnt3a-stimulated luciferase activity (supplementary material Fig. S3), confirming that the extracellular domain is necessary to inhibit exogenous Wnt/β-catenin signalling.

In contrast to our zebrafish studies, Ptk7ECD inhibited luciferase activity to the same extent as full-length protein in HEK293T cultures (supplementary material Fig. S3). This suggests functional differences between *in vivo* and *in vitro* Wnt overexpression systems. Of note, overexpression of Ptk7 extracellular fragments in zebrafish embryos had no effect on patterning and morphogenesis (supplementary material Fig. S4B), whereas Ptk7ΔICD, in which the extracellular domain remains tethered to the plasma membrane, produced both PCP and dorsoventral patterning phenotypes at frequencies similar to full-length Ptk7 (supplementary material Fig. S4B).

Generation of *ptk7* mutant zebrafish

To determine the requirement for Ptk7 in zebrafish embryonic patterning and morphogenesis, we targeted mutations into the genomic *ptk7* locus using specifically engineered ZFNs. Web-based ZiFiT software (http://zifit.partners.org/ZiFiT/) was used to identify an optimal target site within the N-terminus of the pseudokinase domain, upstream from the predicted ATP-binding pocket. OPEN (Oligomerized Pool ENgineering) combinatorial-based selection methods were employed to generate multiple ZFNs (Maeder et al., 2008; Foley et al., 2009), and efficient/specific binding proteins were selected using a bacterial one-hybrid screen (Meng et al., 2008). mRNA (80 pg) coding for each of two ZFN pairs was injected into one-cell stage embryos, F0 fish were raised to adulthood, and F1 genomic DNA was screened for mutations in *ptk7* using PCR-based assays (Fig. 3B). Using this strategy, we isolated a mutant allele ($ptk7^{hsc9}$) harbouring a 10-bp deletion that results in a frame shift and the incorporation of multiple premature termination codons.

In contrast to mouse and *Xenopus* studies, $Ptk7^{hsc9}$ mutant zebrafish develop normally until 3-4 weeks post-fertilisation, at which time mutant larvae acquire axial curvatures (100%, *n*=34; Fig. 3C,D). The presence of significant maternal *ptk7* transcript in homozygous mutant embryos, however, led us to consider the

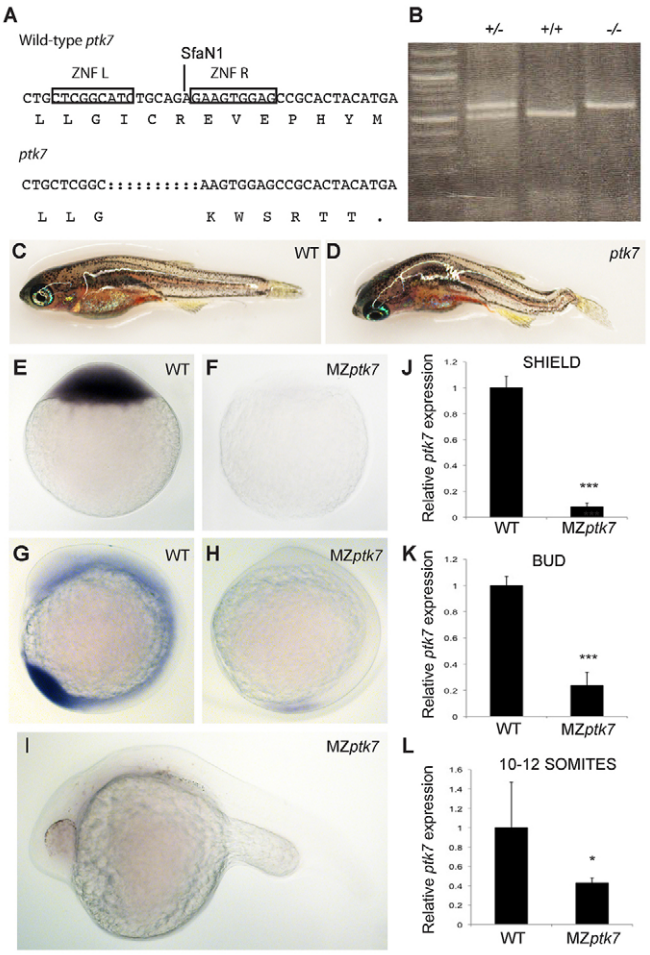

Fig. 3. *Ptk7*^{hsc9} mutant transcript is targeted for non-sense-mediated decay (NMD). (**A**) *Ptk7* ZFN target sequence and *ptk7*^{hsc9} mutant allele. Both the nucleotide and protein sequence are represented. *Ptk7* ZFNs induced a 10-bp deletion, represented by dashed lines in the mutant sequence. This frame-shift mutation yields a premature termination codon immediately adjacent to the target site. Boxes outline the nucleotide target of left (ZFN L) and right (ZFN R) zinc-finger proteins. *Sfa*N1 indicates the restriction site used to identify potential mutations. (**B**) Mutations were identified by PCR amplification of genomic DNA followed by *Sfa*N1 restriction digest. Examples of wild-type (+/+), heterozygote (+/–) and mutant (–/–) zebrafish are represented. The *Ptk7*^{hsc9} allele is not targeted by *Sfa*N1, and runs higher on a DNA gel than wild-type *ptk7*. (**C**,**D**) Wild-type (C) and zygotic *ptk7*^{hsc9} mutant (D) zebrafish at 2 months post-fertilisation. Axial curvatures were observed in 100% of *ptk7*^{hsc9} mutant juvenile and adult zebrafish. (**E-I**) *ptk7* expression in wild-type (E,G) and maternal-zygotic *ptk7*^{hsc9} (MZ*ptk7*^{hsc9}) mutant (F,H,I) embryos, as visualised by WISH at the one-cell (E,F), 10- to 12-somite (G,H) and 24 hpf (I) stages. (**J-L**) Quantitative RT-PCR (qRT-PCR) reveals a strong reduction in *ptk7* transcript in MZ*ptk7*^{hsc9} relative to wild-type at shield (J; ***P<0.001), bud (K; ***P<0.001) and 10- to 12-somite (L; *P=0.0358) stages. Error bars represent the s.e. for the expression level fold change.

possibility that maternal contribution might rescue early developmental defects.

MZptk7^{hsc9} mutant embryos demonstrate loss of Ptk7 function

Maternal zygotic *ptk7*^{hsc9} (MZ*ptk7*^{hsc9}) mutant embryos were generated through routine crosses of *Ptk7*^{hsc9} mutant adults. Because the *ptk7*^{hsc9} mutation introduces multiple premature termination codons into exon 16 of 20, we investigated whether mutant transcript was targeted by non-sense-mediated decay (NMD). Using WISH and qRT-PCR, we did not detect *ptk7* transcripts in one-cell-stage MZ*ptk7*^{hsc9} embryos (100%, n=15; Fig. 3E,F), suggesting strong loss of maternal contribution. At gastrula to early segmentation stages, we observed significant downregulation of *ptk7*^{hsc9} transcript levels (Fig. 3J-L). We did detect small amounts of *ptk7* in the tailbud of 10- to 12-somite-stage MZ*ptk7*^{hsc9} mutants (Fig. 3G,H); however, at 24 hpf, no transcript was observed (Fig. 3I). Our data suggest that *ptk7*^{hsc9} transcripts are subject to NMD, indicating a strong loss-of-function allele.

Ptk7 is required for planar cell polarity

MZ*ptk7*^{hsc9} embryos appear shorter and wider than wild-type embryos (100%, n=100; Fig. 4A-D), indicating possible defects in PCP-mediated C&E movements. Morphometric analyses of *myoD* (*myod1*; somite) and *krox20* (*egr2*; hindbrain) marker expression confirmed a significant compression of the MZ*ptk7*^{hsc9} rostral-caudal axis (Fig. 4E), with concomitant expansion of the MZ*ptk7*^{hsc9} mediolateral axis (Fig. 4F). At tailbud stages, the neural plate and notochord of MZ*ptk7*^{hsc9} embryos (marked by *dlx3* and *ntl* expression, respectively) are expanded mediolaterally, and the prechordal plate (*hgg1*; *ctsl1b*) does not extend to its normal anterior position (100%, n=16; Fig. 4G-J). Furthermore, MZ*ptk7*^{hsc9} embryos demonstrate neural tube morphogenesis defects similar to those observed in MZ*vangl2* embryos (a core PCP signalling mutant) (Ciruna et al., 2006), with cells accumulating ectopically at the neural midline (Fig. 4K,L). Although MZ*ptk7*^{hsc9} embryos are viable through pharyngula and hatching stages, the majority die at 1-2 weeks post-fertilisation. Surviving MZ*ptk7*^{hsc9} adult zebrafish (9%, n=90) appear similar to zygotic *ptk7*^{hsc9} mutant parents.

Cells engaged in C&E movements become elongated and oriented mediolaterally (Keller et al., 2000; Topczewski et al., 2001). Using confocal microscopy, we analysed the shape and orientation of MZ*ptk7*^{hsc9} and wild-type gastrulae cells (Fig. 4M-O). In the dorsal ectoderm of wild-type gastrulae, cells are elongated [length-to-width ratio (LWR) of 2.0±0.46, n=74; Fig. 4M] with strong mediolateral bias in their orientation with respect to the midline (72% of cells within ±15° with respect to the mediolateral axis; Fig. 4N,O). MZ*ptk7*^{hsc9} mutant cells were significantly less elongated (LWR of 1.2±0.24, n=94, P<0.001; Fig. 4M) and exhibited less mediolateral bias in their orientation (22% of cells, P<0.001; Fig. 4N,O), consistent with a loss of PCP.

To investigate further how loss of Ptk7 affects PCP, we visualised the subcellular localisation of GFP-tagged Prickle (GFP-Pk), a cytosolic effector protein that localises asymmetrically along the anterior membrane of zebrafish neuroepithelial and mesodermal cells in response to PCP signals (Carreira-Barbosa et al., 2003; Veeman et al., 2003; Ciruna et al., 2006; Yin et al., 2008). Although GFP-Pk localised to discrete puncta at the anterior plasma membrane of wild-type neuroepithelial cells (47/61 cells, n=4 embryos; Fig. 4P-R), GFP-Pk puncta were largely lost from the anterior membrane in MZ*ptk7*^{hsc9} mutants (puncta present in 2/136 cells, n=6 embryos; Fig. 4P-R). Our results suggest a conserved requirement for Ptk7 in regulating PCP.

Ptk7 potentiates non-canonical Wnt signals

Both hyperactivation and loss of PCP signalling often yield similar embryonic phenotypes (Moon et al., 1993; Park and Moon, 2002; Carreira-Barbosa et al., 2003). To determine whether Ptk7 plays a positive or negative role in PCP, we examined the effect of *ptk7* overexpression on exogenous non-canonical Wnt activity. Although

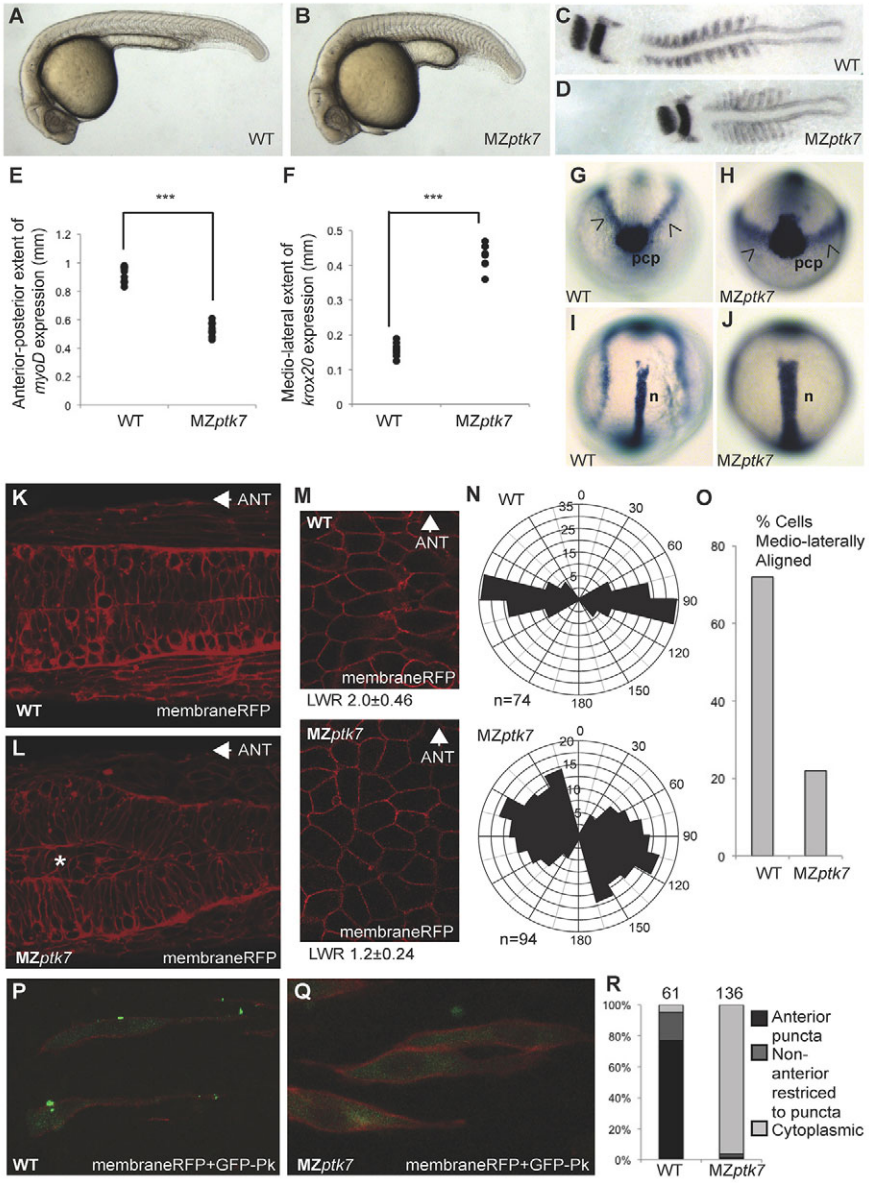

Fig. 4. MZ*ptk7* mutant embryos display PCP-mediated morphogenesis defects. (**A**,**B**) Lateral views of wild-type (A) and MZ*ptk7*^{hsc9} mutant (B) embryos at 24 hpf. (**C**,**D**) Flat-mounts of 10- to12 somite-stage wild-type (C) and MZ*ptk7*^{hsc9} (D) embryos stained for *krox20* (hindbrain) and *myoD* (somite) gene expression. (**E**) Quantification of the anterior-posterior extent of the *myoD* expression domain in wild-type (WT) versus MZ*ptk7*^{hsc9} mutant embryos (***P<0.001, n=8 for each group). (**F**) Quantification of the mediolateral extent of *krox20* expression in WT versus MZ*ptk7*^{hsc9} mutant embryos (***P<0.001, n=8 for each group). MZ*ptk7*^{hsc9} mutant embryos display clear defects in axial extension. (**G-J**) Anterior (G,H) and dorsal (I,J) views of bud stage WT (G,I) and MZ*ptk7*^{hsc9} (H,J) embryos stained for *hgg1* (prechordal plate, pcp), *dlx3* (prospective neural plate, arrowheads) and *ntl* (prospective notochord, n). MZ*ptk7*^{hsc9} mutants demonstrate defects in the convergence of both neuroectoderm and axial mesoderm tissues. (**K**,**L**) Dorsal confocal images of the neural tube and adjacent somites of 24 hpf wild-type (K) and MZ*ptk7*^{hsc9} (L) embryos, injected with membrane-localised monomeric RFP (membraneRFP) (Megason and Fraser, 2003). MZ*ptk7*^{hsc9} mutant embryos display an accumulation of neural progenitors (asterisk in L) at the centre of the neural primordium. Anterior is left. (**M**) MembraneRFP-labelled cells in the dorsal ectoderm of WT and MZ*ptk7*^{hsc9} embryos at 90% epiboly. Dorsal view, midline to the right and anterior to the top. The length-to-width (LWR) ratio of cells are as indicated for WT (n=74) and MZ*ptk7*^{hsc9} (n=94). (**N**) Rose diagrams for cell orientation relative to the embryonic midline at 90% epiboly in WT and MZ*ptk7*^{hsc9} embryos. (**O**) Graph showing percentage of mediolaterally aligned cells, for which longitudinal axis is oriented ±15° with respect to the embryonic mediolateral axis. (**P**,**Q**) Dorsal confocal images of the neural keel and adjacent somites of 8- to 10-somite-stage WT (P) and MZ*ptk7*^{hsc9} (Q) embryos scatter-labelled with GFP-Prickle (GFP-Pk) and membrane RFP. The subcellular localisation of the PCP marker GFP-Pk is disrupted in MZ*ptk7*^{hsc9}. Anterior is up. Confocal imaging was carried out at the level of the first to the fifth somite pairs. (**R**) Quantification of the localisation of GFP-Pk puncta in WT (four embryos) versus MZ*ptk7*^{hsc9} (six embryos).

injection of high levels of *wnt5* (Kilian et al., 2003) or *ptk7* (Fig. 2A-C) mRNA interfere with zebrafish C&E movements, injection of low *wnt5b* or *ptk7* mRNA levels do not disrupt embryonic morphogenesis (Fig. 5A,B). Strikingly, we observed that co-expression of low levels of both *wnt5b* and *ptk7* mRNA yielded strong defects in C&E, as quantified through morphometric analyses of *myoD* expression (Fig. 5A,B). This observation suggests that Ptk7 potentiates Wnt5 signalling activity *in vivo*.

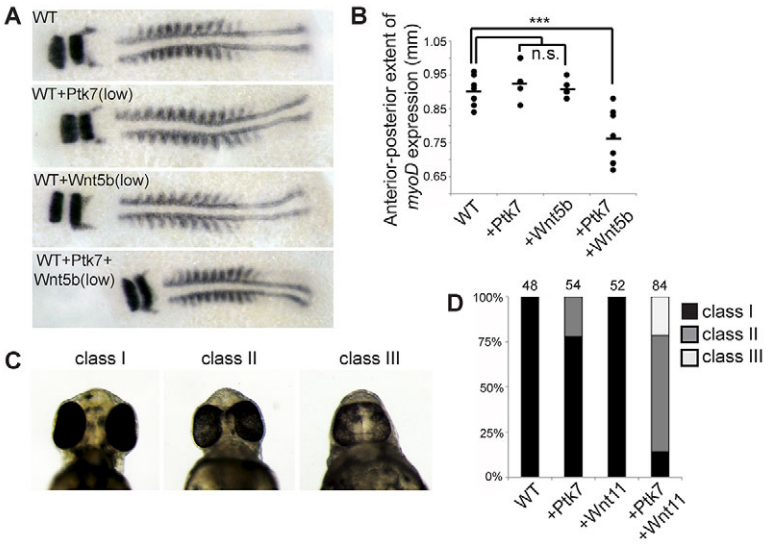

Fig. 5. *Ptk7* overexpression inhibits exogenous non-canonical Wnt/PCP activity. (**A**) Flat-mounts of 10- to 12-somite stage wild-type (WT) embryos and embryos injected with *ptk7* (200 pg), *wnt5b* (50 pg) or *ptk7* (200pg) + *wnt5b* (50 pg) mRNA stained for *krox20* (hindbrain) and *myoD* (somite) gene expression. (**B**) Quantification of the anterior-posterior extent of the *myoD* expression domain in WT, *ptk7* (200 pg), *wnt5b* (50 pg), and *ptk7* (200 pg) + *wnt5b* (50 pg) mRNA-injected embryos (***P<0.001). n.s., not significant. (**C**) Ventral views of embryos at 2 days post-fertilisation (dpf). Cyclopia phenotypes were observed as class I (no cyclopia), class II (partial cyclopia) and class III (full cyclopia). (**D**) Quantification of cyclopia phenotypes in WT, *ptk7* (200 pg), *wnt11* (50 pg), and *ptk7* (200 pg) + *wnt11* (50 pg) mRNA-injected embryos at 2 dpf.

Similarly, embryos injected with high levels of *wnt11* mRNA displayed cyclopia (a phenotype associated with activated non-canonical Wnt signalling) (Ungar et al., 1995; Lu et al., 2011), whereas injection of lower *wnt11* mRNA levels did not adversely affect embryogenesis (Fig. 5C,D). However, we observed that co-injection of *ptk7* mRNA with low levels of *wnt11* mRNA caused a striking increase in both the incidence and severity of cyclopia, as scored in live embryos at 48 hpf (Fig. 5C,D). The synergistic effect of exogenous *ptk7* and *wnt11* expression on PCP-mediated morphogenetic processes suggests that Ptk7 regulates PCP by potentiating non-canonical Wnt signal activity.

MZ*ptk7*^{hsc9} mutants display subtle dorsoventral patterning defects

We have also shown that overexpression of *ptk7* attenuates Wnt/β-catenin signalling, suggesting an inhibitory role for Ptk7 in canonical Wnt signal transduction (Fig. 2). However, MZ*ptk7*^{hsc9} mutant embryos do not display the gross embryological defects typically associated with mis-regulated Wnt/β-catenin activity, such as dorsalisation, ventralisation, or mispatterning of the CNS (supplementary material Fig. S5).

To investigate further the role for Ptk7 in dorsoventral patterning, we used qRT-PCR to quantify β-catenin-dependent dorsal organiser gene expression in wild-type versus MZ*ptk7*^{hsc9} mutant embryos. At 4 hpf, we observed a small but significant upregulation of *bozozok* (*boz*) and *chordin* (*chd*) expression in MZ*ptk7*^{hsc9} mutants (Fig. 6A), suggesting an inhibitory role for *ptk7* in dorsal organiser formation. MZ*ptk7*^{hsc9} mutants also demonstrated a slight expansion in *boz* expression at 50% epiboly as detected by WISH (100%, n=20) and qRT-PCR (Fig. 6B). However, by gastrulation, we could no longer detect significant differences in the dorsal expression of *chd* and *goosecoid* (*gsc*) (Fig. 6C,D), nor did we observe changes in ventral *axin2* or *vox* expression (Fig. 6C,D). Therefore, although *ptk7* might play a role in restricting dorsal organiser formation, genetic loss of *ptk7* does not have a significant effect on subsequent establishment and/or maintenance of dorsoventral domains in the zebrafish gastrula.

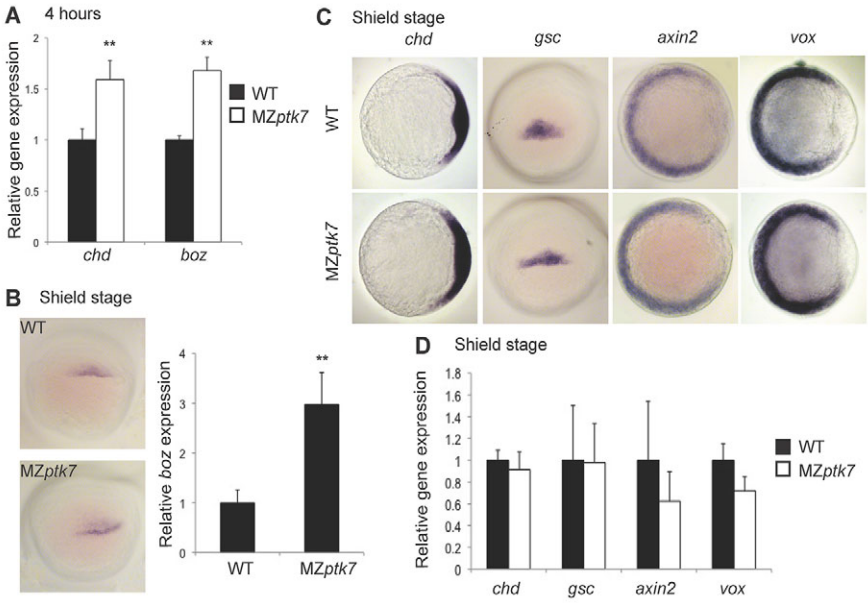

Fig. 6. MZ*ptk7*^{hsc9} embryos establish normal dorsoventral pattern. (**A**) *Chordin* (*chd*) and *bozozok* (*boz*) expression is slightly increased in MZ*ptk7*^{hsc9} embryos immediately following MBT, as assayed by qRT-PCR of embryos at 4 hpf. **P<0.01. (**B**) *Boz* expression is increased in MZ*ptk7*^{hsc9} embryos prior to gastrulation as assayed by WISH (dorsal view), and by qRT-PCR at 50% epiboly (**P=0.0078). (**C**) Whole-mount *in situ* hybridisation (WISH) for dorsal organiser genes *chordin* (*chd*) and *goosecoid* (*gsc*), and ventral genes *axin2* and *vox* at shield stage. Embryos are viewed from the animal pole with dorsal to the right (for *chd*, *axin2* and *vox*). *gsc* expression is shown as a dorsal view. (**D**) qRT-PCR assays of *chd* (P=0.4675), *gsc* (P=0.9515), *axin2* (P=0.07) and *vox* (P=0.3974) expression in wild-type (WT) versus MZ*ptk7*^{hsc9} embryos at shield stage. No significant differences in gene expression were observed. Error bars represent the s.e. for the expression level fold change.

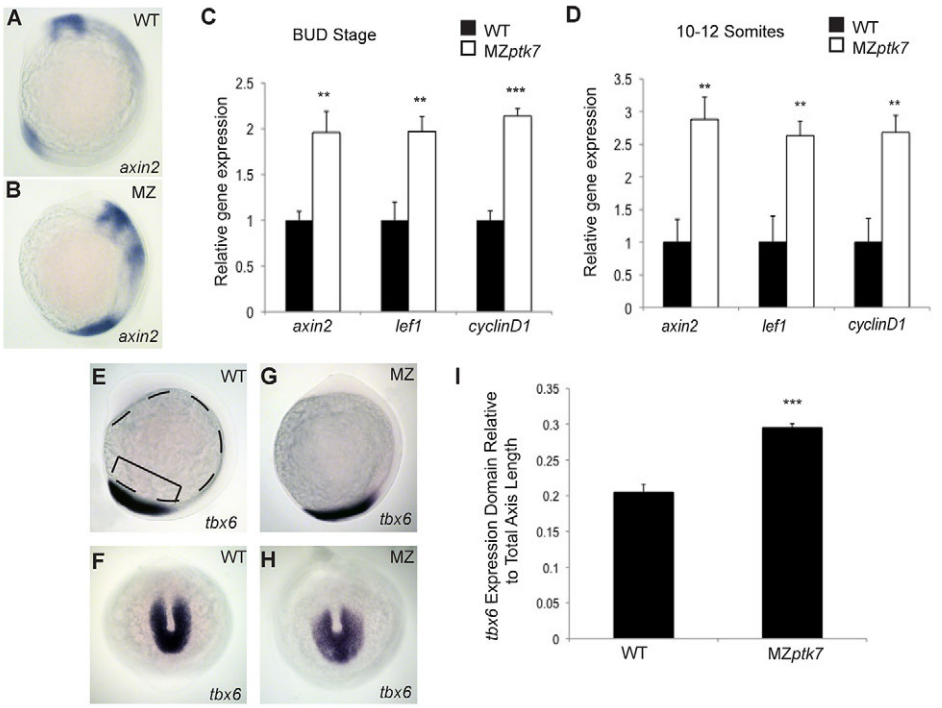

Fig. 7. *Ptk7* is required to attenuate Wnt/β-catenin signalling in the vertebrate tailbud. (**A**,**B**) Whole-mount *in situ* hybridisation of a*xin2* expression in 10- to 12-somite stage wild-type (A) and MZ*ptk7*^{hsc9} (B) embryos. (**C**,**D**) qRT-PCR indicates upregulated Wnt-target gene expression in MZ*ptk7*^{hsc9} embryos. (C) Bud stage expression of *axin2* (**P=0.0026), *lef1* (**P=0.0028) and *cyclin D1* (***P<0.0001) in MZ*ptk7*^{hsc9} relative to wild type (WT). (D) Expression at the 10-12 somite stage of *axin2* (**P=0.0026), *lef1* (**P<0.0035) and *cyclin D1* (**P=0.0028) in MZ*ptk7*^{hsc9} relative to WT. (**E-H**) Lateral (E,G) and tailbud (F,H) views of Wnt/β-catenin-dependent *tbx6* expression in WT (E,F) and MZ*ptk7*^{hsc9} mutant (G,H) embryos. (**I**) Quantification of the size of the *tbx6* expression domain (bracket, E) relative to the total embryonic body length (dashed line, E) in WT and MZ*ptk7*^{hsc9} mutant embryos. The *tbx6*-positive presomitic mesoderm domain is significantly expanded in MZ*ptk7*^{hsc9} mutants. ***P<0.001. Error bars represent the s.e. for the expression level fold change for qRT-PCR and s.d. in I.

Ptk7 regulates Wnt/β-catenin-dependent cell fate decisions in the vertebrate tailbud

Post-gastrulation, Wnt/β-catenin signalling is required for posterior vertebrate axis development (Galceran et al., 1999; Agathon et al., 2003; Martin and Kimelman, 2008), and drives an ongoing process of mesodermal fate specification within stem cell pools of the tailbud (Martin and Kimelman, 2012). As *ptk7* expression is highly enriched in the tailbud, we investigated the post-gastrula role for Ptk7 in canonical Wnt/β-catenin activity. Using WISH, we observed upregulated levels of *axin2* expression within the presomitic mesoderm of 10- to 12-somite stage MZ*ptk7*^{hsc9} embryos (100%, n=17; Fig. 7A,B). Furthermore, *axin2*, *lef1* and *cyclin D1* expression levels were all significantly upregulated in MZ*ptk7*^{hsc9} embryos at both bud and 10- to 12-somite stages, as assayed by qRT-PCR (Fig. 7C,D). Our data indicate that Ptk7 is required to attenuate canonical Wnt/β-catenin signal transduction in the developing tailbud.

To determine whether Ptk7 regulates canonical Wnt-dependent cell fate decisions in the tailbud, we used WISH to examine *tbx6* expression (a direct target of Wnt/β-catenin signals, and a marker of presomitic mesoderm) in control versus MZ*ptk7*^{hsc9} mutant embryos. Strikingly, the *tbx6* expression domain was expanded in the tailbud of 10- to 12-somite stage MZ*ptk7*^{hsc9} embryos (Fig. 7E-I). Similarly, WISH analysis of *mespb* expression (which defines the anterior limit of presomitic mesoderm) also revealed a rostral extension in the MZ*ptk7*^{hsc9} presomitic mesoderm domain, and a significant expansion of the tailbud (supplementary material Fig. S6).

To determine whether observed patterning defects are an artefact of abnormal PCP-mediated tailbud morphogenesis, we examined Wnt/β-catenin target gene expression and mesodermal fate specification in *vangl2* mutant embryos. No significant differences in *axin2*, *lef1* or *cyclin D1* expression were observed (supplementary material Fig. S7A), indicating that loss of PCP is not sufficient to promote canonical Wnt/β-catenin activity. Furthermore, no significant expansion of *tbx6* expression was observed within the tailbud of *vangl2* mutants (supplementary material Fig. S7B,C). Our data suggest that the expansion of mesodermal fate observed in MZ*ptk7*^{hsc9} embryos is not a consequence of abnormal PCP. Rather, our data further supports the role for Ptk7 as an inhibitor of the Wnt/β-catenin signalling pathway, with essential functions in regulating canonical Wnt-dependent cell fate decisions in posterior stem cell pools of the vertebrate tailbud.

Ptk7 activity can be rescued with membrane-tethered extracellular domain

In contrast to MZ*ptk7*^{hsc9} mutants, zygotic *ptk7* mutant embryos appear normal. This indicates that maternal *ptk7*, which is present at the one-cell stage, is sufficient to rescue embryonic patterning and morphogenesis through to juvenile stages. We therefore reasoned that careful titration of *ptk7* mRNA into one-cell-stage embryos might rescue MZ*ptk7*^{hsc9} embryogenesis. Indeed, injection of full-length *ptk7* mRNA constructs could largely rescue both C&E (Fig. 8A) and tailbud patterning defects (Fig. 8B) associated with MZ*ptk7*^{hsc9} mutant embryos. Therefore, we decided to perform structure-function analysis of Ptk7 by assaying the differential ability of deletion and substitution constructs to rescue MZ*ptk7*^{hsc9} mutant phenotypes.

The kinase domain of Ptk7, which interacts with Dvl, RACK1 and β-catenin, is thought to be essential for Ptk7 activity despite an apparent lack of catalytic activity (Lu et al., 2004; Shnitsar and Borchers, 2008; Puppo et al., 2011). Moreover, *Xenopus* overexpression studies suggest that Ptk7 kinase deletion mutants possess dominant-negative activity, disrupting both PCP C&E movements (Lu et al., 2004; Shnitsar and Borchers, 2008) and Wnt/β-catenin dorsal organiser gene expression (Puppo et al., 2011). However, we found that zebrafish *ptk7ΔICD* expression constructs (lacking the entire intracellular domain) rescued both MZ*ptk7*^{hsc9} axial extension and *tbx6* tailbud patterning defects to the same extent as did full-length *ptk7* expression (Fig. 8A,B). Similarly, we found that *ptk7EgfrTM* expression (substituting the transmembrane domain for that of Egfr) also rescued MZ*ptk7*^{hsc9} patterning and

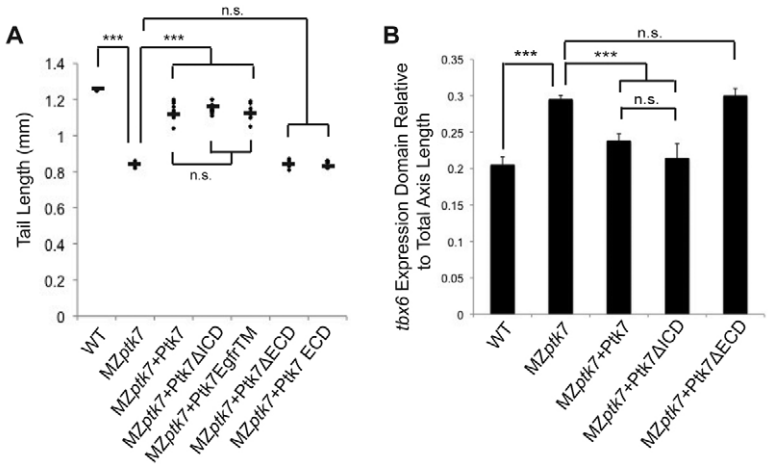

Fig. 8. The extracellular domain of Ptk7 is sufficient for activity. Ptk7 structure-function analysis, assaying the ability of Ptk7 mutant isoforms to rescue axial extension (A) and tailbud patterning (B) defects of MZ*ptk7*^{hsc9} mutant embryos. (**A**) Quantification of tail length measured from the base of the yolk extension to the tail tip of wild-type (WT), MZ*ptk7*, MZ*ptk7*+*ptk7* (300 pg) mRNA, MZ*ptk7*+*ptk7ΔICD* (200 pg) mRNA, MZ*ptk7*+*ptk7egfrTM* (300 pg) mRNA, MZ*ptk7*+ *ptk7ΔECD* (150 pg) mRNA, and MZ*ptk7*+*ptk7 ECD* (200 pg) mRNA-injected embryos. Ptk7ΔECD and Ptk7 ECD cannot rescue the body axis defect in MZ*ptk7*^{hsc9}. Each point represents a single embryo, horizontal lines represent the mean of each group. *n*=10 for each group. ***P<0.001. (**B**) Quantification of the size of the *tbx6* expression domain relative to the total embryonic body length in WT, MZ*ptk7*, MZ*ptk7*+*ptk7* (300 pg) mRNA, MZ*ptk7*+*ptk7ΔICD* (200 pg) mRNA, and MZ*ptk7*+ *ptk7ΔECD* (150 pg) mRNA-injected embryos. *Tbx6* expression is expanded in MZ*ptk7*. This can be rescued by full-length Ptk7 and Ptk7ΔICD but not by Ptk7ΔECD. ***P<0.001. n.s., not significant. Error bars represent s.d.

morphogenesis (Fig. 8A,B). Our results indicate that the pseudokinase domain of Ptk7 is not required for non-canonical/PCP or canonical Wnt/β-catenin signalling activity.

However, deletion of the Ptk7 extracellular domain (*ptk7ΔECD*) abrogated its ability to rescue MZ*ptk7*^{hsc9} axial extension and mesodermal fate specification defects (Fig. 8A), indicating a clear requirement for the extracellular domain in regulating PCP and Wnt/β-catenin signal transduction. Of interest, expression of a secreted Ptk7 extracellular fragment (*ptk7ECD*) failed to rescue MZ*ptk7*^{hsc9} mutant phenotypes (Fig. 8A,B). Therefore, our results clearly indicate that the plasma membrane-tethered extracellular domain of Ptk7 is both required and sufficient to regulate PCP-mediated morphogenesis and Wnt/β-catenin cell fate decisions during zebrafish embryonic development.

DISCUSSION

The Wnt pathway comprises a complex network of signalling molecules, which integrate extracellular information using multiple cell surface proteins. The presence or absence of a single component can dictate the context of cellular response, favouring activation of canonical Wnt/β-catenin, non-canonical Wnt/PCP, or other alternative Wnt signalling pathways. Recent studies implicate Ptk7 as a novel Wnt co-receptor that can influence signal specificity during vertebrate embryogenesis. However, conflicting reports have indicated both positive and negative roles for Ptk7 in regulating Wnt/β-catenin activity.

In this study, we cloned and characterised the zebrafish *ptk7* orthologue. Zebrafish *ptk7* is strongly expressed in one-cell-stage embryos, it is expressed ubiquitously throughout gastrulation, and strong *ptk7* expression is maintained in the tailbud throughout segmentation stages. Using ZFNs assembled through OPEN combinatorial-based selection methods (Maeder et al., 2008; Foley et al., 2009), we generated a *ptk7* mutant allele (hsc9) containing a 10-bp deletion within the pseudokinase domain. *ptk7*^{hsc9} transcript is subject to non-sense-mediated decay, indicating a strong loss-of-function allele.

Ptk7 and non-canonical Wnt/PCP signalling

Zygotic *ptk7*^{hsc9} mutant embryos develop normally, with no appreciable defects in embryonic patterning or morphogenesis. However, maternal zygotic *ptk7*^{hsc9} mutant embryos display axial C&E defects, abnormal neural tube morphogenesis, and loss of PCP. Our results provide further evidence that Ptk7 is an essential regulator of vertebrate PCP. More importantly, we demonstrate that Ptk7 enhances the activity of exogenous Wnt5 and Wnt11 ligands, indicating that Ptk7 regulates PCP by potentiating non-canonical Wnt signal transduction.

Although the molecular mechanisms by which Ptk7 promotes PCP remain ill defined, overexpression studies in *Xenopus* have implicated a key role for the highly conserved Ptk7 pseudokinase domain: it interacts with receptor of activated protein kinase C 1 [RACK1, a known effector of Dvl required for *Xenopus* neural tube closure (Wehner et al., 2011; Kinoshita et al., 2003)], and it is required for Ptk7-mediated translocation (and subsequent hyper-phosphorylation) of Dvl to the plasma membrane (Shnitsar and Borchers, 2008). In this study, we used an *in vivo* rescue-based strategy to perform structure-function analyses of Ptk7. Strikingly, we found that full-length Ptk7 and Ptk7ΔICD constructs have equivalent abilities to rescue MZ*ptk7*^{hsc9} C&E defects, whereas deletion of the Ptk7 extracellular domain eliminated protein function. Therefore, the kinase domain is dispensable for Ptk7 activity in PCP-directed C&E. Rather, our data indicates that a plasma membrane-tethered Ptk7 extracellular domain (Ptk7ΔICD) is sufficient to promote normal PCP, and highlights the importance of extracellular protein-protein interactions for Ptk7 function.

Our findings complement recent studies of mammalian Ptk7, which demonstrate that Ptk7 is not required for Dvl2 membrane localisation in planar polarised cells of the mouse mesoderm or auditory epithelium (Yen et al., 2009; Lee et al., 2012). Therefore, functions for the Ptk7 kinase domain in Dvl localisation and PCP might have evolved differently in *Xenopus*. Alternatively, Ptk7 might have context-dependent PCP functions. The specific role for Ptk7 intracellular domains in oriented cell division (Gong et

al., 2004), radial intercalation (Roszko et al., 2009), cilia orientation (Borovina et al., 2010; Happé et al., 2011), and facial branchiomotor neuron migration (Jessen et al., 2002) remain to be determined.

Ptk7 and canonical Wnt/β-catenin activity

We have demonstrated that overexpression of zebrafish Ptk7 disrupts dorsoventral patterning, inhibits Wnt/β-catenin-dependent gene expression in early gastrula-stage embryos and inhibits the effects of *wnt8* overexpression. Furthermore, loss of Ptk7 activity in MZ*ptk7*^{hsc9} mutant embryos results in increased Wnt/β-catenin target gene transcription at early segmentation stages. *Ptk7* is strongly expressed in the tailbud, where Wnt/β-catenin signals specify paraxial mesoderm cell fate from bi-potential neural/mesodermal progenitor cell pools (Martin and Kimelman, 2012). In MZ*ptk7*^{hsc9} embryos, we observe an expanded domain of pre-somitic mesoderm differentiation that is independent of PCP-mediated morphogenesis defects. Our data therefore indicate that Ptk7 attenuates Wnt/β-catenin signalling during vertebrate embryogenesis, with essential roles in regulating Wnt/β-catenin-dependent stem cell fate decisions in the developing tailbud.

Wnt/β-catenin patterning defects have not been reported in three independent analyses of *Ptk7* mutant mice (Lu et al., 2004; Yen et al., 2009; Paudyal et al., 2010). However, these studies focused predominantly on PCP-related phenotypes. Of note, Paudyal et al. (Paudyal et al., 2010) did report a shortened spinal cord and body axis in *chuzoi* Ptk7 mutant mouse embryos, which would be consistent with misregulated Wnt/β-catenin signalling during posterior paraxial mesoderm differentiation and tailbud outgrowth.

In *Xenopus*, studies of Ptk7 function using antisense MO methodologies have yielded conflicting results. Peradziryi et al. (Peradziryi et al., 2011) demonstrated that knockdown of Ptk7 in animal cap explants stimulated β-catenin target gene transcription in response to exogenous Wnt signals. This study supports our findings that Ptk7 inhibits Wnt/β-catenin signalling *in vivo*; however, endogenous Wnt/β-catenin patterning defects were not reported for *Xenopus PTK7* MO-injected embryos. In a second study, MO knockdown of PTK7 activity caused defects in Spemann organiser formation, suggesting that Ptk7 potentiates canonical Wnt signalling (Puppo et al., 2011). Although this finding is difficult to reconcile with our analysis of MZ*ptk7*^{hsc9} mutant embryos, PCP factors such as Vangl2 have been implicated in the asymmetric distribution of maternal transcripts within *Xenopus* oocytes, which is required for dorsoventral pattern formation (Cha et al., 2011). As Ptk7 is a well-established regulator of PCP, defects observed in the latter study may reflect a similar requirement for maternal Ptk7 in *Xenopus* oocyte polarity.

Of interest, despite an early expansion of Wnt/β-catenin-dependent dorsal organiser gene expression in MZ*ptk7*^{hsc9} mutant embryos, we did not observe later dorsoventral or anterior CNS patterning defects. As Wnt/β-catenin signals also restrict dorsal organiser activity in later-staged blastula, it is possible that potentiation of ventralising Wnt/β-catenin signals in MZ*ptk7*^{hsc9} mutants might compensate for early expansion of the dorsal organiser. Alternatively, there may be functional redundancy between Ptk7 and other Wnt/β-catenin inhibitors (van de Water et al., 2001; Kagermeier-Schenk et al., 2011; Xie et al., 2011). For example, the transmembrane protein Waif1 has recently been shown to attenuate Wnt/β-catenin signalling while promoting PCP (Kagermeier-Schenk et al., 2011). Zebrafish *waif1* (also known as *tpbg*) is broadly expressed during gastrulation but becomes restricted to the neuroectoderm during segmentation (Kagermeier-Schenk et al., 2011) and these domains overlap with *ptk7* expression.

We have also demonstrated that the Ptk7 pseudokinase domain is dispensable for Wnt/β-catenin signal inhibition, as assayed by rescue of MZ*ptk7*^{hsc9} tailbud patterning defects. Rather, a plasma membrane-tethered Ptk7 extracellular domain is sufficient for this activity. Our results contrast recent work by Puppo et al. (Puppo et al., 2011), which suggests that physical interactions between the pseudokinase domain and intracellular β-catenin might provide a mechanistic link between Ptk7 and canonical Wnt signal transduction pathways. However, Ptk7 can form a complex with Fz (Shnitsar and Borchers, 2008; Peradziryi et al., 2011), and the extracellular domain of Ptk7 can selectively bind canonical ligands Wnt3a and Wnt8 (Peradziryi et al., 2011). This suggests that Ptk7 may function as a canonical Wnt co-receptor to affect pathway specificity *in vivo*. Our work highlights the importance of the Ptk7 extracellular domain in both Wnt/β-catenin and non-canonical Wnt/PCP signal transduction pathways during vertebrate embryonic development.

Ptk7, cancer, congenital malformations and disease

Wnt/β-catenin signalling plays an oncogenic role in the development of colon cancer, hepatocellular carcinoma and multiple other tumours (Clevers, 2006). By contrast, non-canonical Wnt pathways antagonise Wnt/β-catenin signalling, and have been speculated to drive morphogenetic cell behaviours associated with tumour invasion and metastasis – pathogenic events that account for ~90% of cancer deaths (Wang, 2009). Our data demonstrate that Ptk7 not only promotes PCP, but also inhibits Wnt/ β-catenin signalling during vertebrate development. Therefore, our results could have significant implications for Ptk7 misregulation observed in colon carcinoma, AML and multiple other cancer types (Mossie et al., 1995; Easty et al., 1997; Endoh et al., 2004; Müller-Tidow et al., 2004; Gorringe et al., 2005; Golubkov et al., 2010; Prebet et al., 2010; Gobble et al., 2011). For example, during cancer progression Ptk7 could initiate a switch from β-catenin-mediated tumour formation and cell proliferation towards PCP-directed changes in cell adhesion, polarity and motility that are associated with metastasis.

Zygotic *ptk7*^{hsc9} mutant embryos display no obvious defects in embryonic patterning or morphogenesis. Rather, maternal Ptk7 is sufficient to rescue early development. This maternal rescue will now permit us to investigate the role for Ptk7 (and consequently, misregulated Wnt/β-catenin and PCP signalling) in juvenile growth, patterning and adult physiology. For example, the late onset of axial deformity observed in zygotic *ptk7*^{hsc9} mutants suggests that they occur independently of early tailbud patterning defects. Indeed, aberrant activation of Wnt/β-catenin signalling has also been implicated in a wide variety of human pathologies (Clevers and Nusse, 2012). Zygotic *ptk7*^{hsc9} mutant zebrafish may therefore prove to be a useful model for determining the consequences of abnormal Wnt signal transduction in adult/late-onset disease.

Acknowledgements

We thank Drs Scot A. Wolfe, Nathan D. Lawson and Keith Joung, the Howard Hughes Medical Institute and Massachusetts Institute of Technology for reagents utilized in the generation of zebrafish *ptk7* ZFNs.

Funding

This work was supported in part by the Canadian Research Chairs program; and by an operating grant from the Canadian Institutes of Health Research [#111075 to B.C.].

Competing interests statement
The authors declare no competing financial interests.

Supplementary material
Supplementary material available online at
http://dev.biologists.org/lookup/suppl/doi:10.1242/dev.090183/-/DC1

References

Agathon, A., Thisse, C. and Thisse, B. (2003). The molecular nature of the zebrafish tail organizer. *Nature* **424**, 448-452.
Angers, S., Thorpe, C. J., Biechele, T. L., Goldenberg, S. J., Zheng, N., MacCoss, M. J. and Moon, R. T. (2006). The KLHL12-Cullin-3 ubiquitin ligase negatively regulates the Wnt-beta-catenin pathway by targeting Dishevelled for degradation. *Nat. Cell Biol.* **8**, 348-357.
Borovina, A., Superina, S., Voskas, D. and Ciruna, B. (2010). Vangl2 directs the posterior tilting and asymmetric localization of motile primary cilia. *Nat. Cell Biol.* **12**, 407-412.
Carreira-Barbosa, F., Concha, M. L., Takeuchi, M., Ueno, N., Wilson, S. W. and Tada, M. (2003). Prickle 1 regulates cell movements during gastrulation and neuronal migration in zebrafish. *Development* **130**, 4037-4046.
Cha, S. W., Tadjuidje, E., Wylie, C. and Heasman, J. (2011). The roles of maternal Vangl2 and aPKC in Xenopus oocyte and embryo patterning. *Development* **138**, 3989-4000.
Chou, Y. H. and Hayman, M. J. (1991). Characterization of a member of the immunoglobulin gene superfamily that possibly represents an additional class of growth factor receptor. *Proc. Natl. Acad. Sci. USA* **88**, 4897-4901.
Ciruna, B., Jenny, A., Lee, D., Mlodzik, M. and Schier, A. F. (2006). Planar cell polarity signalling couples cell division and morphogenesis during neurulation. *Nature* **439**, 220-224.
Clevers, H. (2006). Wnt/beta-catenin signaling in development and disease. *Cell* **127**, 469-480.
Clevers, H. and Nusse, R. (2012). Wnt/β-catenin signaling and disease. *Cell* **149**, 1192-1205.
De Robertis, E. M. and Kuroda, H. (2004). Dorsal-ventral patterning and neural induction in Xenopus embryos. *Annu. Rev. Cell Dev. Biol.* **20**, 285-308.
De Robertis, E. M., Larraín, J., Oelgeschläger, M. and Wessely, O. (2000). The establishment of Spemann's organizer and patterning of the vertebrate embryo. *Nat. Rev. Genet.* **1**, 171-181.
Easty, D. J., Mitchell, P. J., Patel, K., Flørenes, V. A., Spritz, R. A. and Bennett, D. C. (1997). Loss of expression of receptor tyrosine kinase family genes PTK7 and SEK in metastatic melanoma. *Int. J. Cancer* **71**, 1061-1065.
Endoh, H., Tomida, S., Yatabe, Y., Konishi, H., Osada, H., Tajima, K., Kuwano, H., Takahashi, T. and Mitsudomi, T. (2004). Prognostic model of pulmonary adenocarcinoma by expression profiling of eight genes as determined by quantitative real-time reverse transcriptase polymerase chain reaction. *J. Clin. Oncol.* **22**, 811-819.
Fekany, K., Yamanaka, Y., Leung, T., Sirotkin, H. I., Topczewski, J., Gates, M. A., Hibi, M., Renucci, A., Stemple, D., Radbill, A. et al. (1999). The zebrafish bozozok locus encodes Dharma, a homeodomain protein essential for induction of gastrula organizer and dorsoanterior embryonic structures. *Development* **126**, 1427-1438.
Foley, J. E., Yeh, J. R., Maeder, M. L., Reyon, D., Sander, J. D., Peterson, R. T. and Joung, J. K. (2009). Rapid mutation of endogenous zebrafish genes using zinc finger nucleases made by Oligomerized Pool ENgineering (OPEN). *PLoS ONE* **4**, e4348.
Galceran, J., Fariñas, I., Depew, M. J., Clevers, H. and Grosschedl, R. (1999). Wnt3a(-/-)-like phenotype and limb deficiency in Lef1(-/-)Tcf1(-/-) mice. *Genes Dev.* **13**, 709-717.
Gao, B., Song, H., Bishop, K., Elliot, G., Garrett, L., English, M. A., Andre, P., Robinson, J., Sood, R., Minami, Y. et al. (2011). Wnt signaling gradients establish planar cell polarity by inducing Vangl2 phosphorylation through Ror2. *Dev. Cell* **20**, 163-176.
Gobble, R. M., Qin, L. X., Brill, E. R., Angeles, C. V., Ugras, S., O'Connor, R. B., Moraco, N. H., Decarolis, P. L., Antonescu, C. and Singer, S. (2011). Expression profiling of liposarcoma yields a multigene predictor of patient outcome and identifies genes that contribute to liposarcomagenesis. *Cancer Res.* **71**, 2697-2705.
Golubkov, V. S., Chekanov, A. V., Cieplak, P., Aleshin, A. E., Chernov, A. V., Zhu, W., Radichev, I. A., Zhang, D., Dong, P. D. and Strongin, A. Y. (2010). The Wnt/planar cell polarity protein-tyrosine kinase-7 (PTK7) is a highly efficient proteolytic target of membrane type-1 matrix metalloproteinase: implications in cancer and embryogenesis. *J. Biol. Chem.* **285**, 35740-35749.
Gong, Y., Mo, C. and Fraser, S. E. (2004). Planar cell polarity signalling controls cell division orientation during zebrafish gastrulation. *Nature* **430**, 689-693.
Gorringe, K. L., Boussioutas, A. and Bowtell, D. D. (2005). Novel regions of chromosomal amplification at 6p21, 5p13, and 12q14 in gastric cancer identified by array comparative genomic hybridization. *Genes Chromosomes Cancer* **42**, 247-259.
Hamblet, N. S., Lijam, N., Ruiz-Lozano, P., Wang, J., Yang, Y., Luo, Z., Mei, L., Chien, K. R., Sussman, D. J. and Wynshaw-Boris, A. (2002). Dishevelled 2 is essential for cardiac outflow tract development, somite segmentation and neural tube closure. *Development* **129**, 5827-5838.
Happé, H., de Heer, E. and Peters, D. J. (2011). Polycystic kidney disease: the complexity of planar cell polarity and signaling during tissue regeneration and cyst formation. *Biochim. Biophys. Acta* **1812**, 1249-1255.
Ikeya, M., Lee, S. M., Johnson, J. E., McMahon, A. P. and Takada, S. (1997). Wnt signalling required for expansion of neural crest and CNS progenitors. *Nature* **389**, 966-970.
Jenny, A. and Mlodzik, M. (2006). Planar cell polarity signaling: a common mechanism for cellular polarization. *Mt. Sinai J. Med.* **73**, 738-750.
Jenny, A., Darken, R. S., Wilson, P. A. and Mlodzik, M. (2003). Prickle and Strabismus form a functional complex to generate a correct axis during planar cell polarity signaling. *EMBO J.* **22**, 4409-4420.
Jessen, J. R., Topczewski, J., Bingham, S., Sepich, D. S., Marlow, F., Chandrasekhar, A. and Solnica-Krezel, L. (2002). Zebrafish trilobite identifies new roles for Strabismus in gastrulation and neuronal movements. *Nat. Cell Biol.* **4**, 610-615.
Jung, J. W., Shin, W. S., Song, J. and Lee, S. T. (2004). Cloning and characterization of the full-length mouse Ptk7 cDNA encoding a defective receptor protein tyrosine kinase. *Gene* **328**, 75-84.
Kagermeier-Schenk, B., Wehner, D., Ozhan-Kizil, G., Yamamoto, H., Li, J., Kirchner, K., Hoffmann, C., Stern, P., Kikuchi, A., Schambony, A. et al. (2011). Waif1/5T4 inhibits Wnt/β-catenin signaling and activates noncanonical Wnt pathways by modifying LRP6 subcellular localization. *Dev. Cell* **21**, 1129-1143.
Keller, R. (2002). Shaping the vertebrate body plan by polarized embryonic cell movements. *Science* **298**, 1950-1954.
Keller, R., Davidson, L., Edlund, A., Elul, T., Ezin, M., Shook, D. and Skoglund, P. (2000). Mechanisms of convergence and extension by cell intercalation. *Philos. Trans. R. Soc. Lond. B Biol. Sci.* **355**, 897-922.
Kilian, B., Mansukoski, H., Barbosa, F. C., Ulrich, F., Tada, M. and Heisenberg, C. P. (2003). The role of Ppt/Wnt5 in regulating cell shape and movement during zebrafish gastrulation. *Mech. Dev.* **120**, 467-476.
Kinoshita, N., Iioka, H., Miyakoshi, A. and Ueno, N. (2003). PKC delta is essential for Dishevelled function in a noncanonical Wnt pathway that regulates Xenopus convergent extension movements. *Genes Dev.* **17**, 1663-1676.
Kohn, A. D. and Moon, R. T. (2005). Wnt and calcium signaling: beta-catenin-independent pathways. *Cell Calcium* **38**, 439-446.
Lee, S. T., Strunk, K. M. and Spritz, R. A. (1993). A survey of protein tyrosine kinase mRNAs expressed in normal human melanocytes. *Oncogene* **8**, 3403-3410.
Lee, J., Andreeva, A., Sipe, C. W., Liu, L., Cheng, A. and Lu, X. (2012). PTK7 regulates myosin II activity to orient planar polarity in the mammalian auditory epithelium. *Curr. Biol.* **22**, 956-966.
Lekven, A. C., Thorpe, C. J., Waxman, J. S. and Moon, R. T. (2001). Zebrafish wnt8 encodes two wnt8 proteins on a bicistronic transcript and is required for mesoderm and neurectoderm patterning. *Dev. Cell* **1**, 103-114.
Logan, C. Y. and Nusse, R. (2004). The Wnt signaling pathway in development and disease. *Annu. Rev. Cell Dev. Biol.* **20**, 781-810.
Lu, X., Borchers, A. G., Jolicoeur, C., Rayburn, H., Baker, J. C. and Tessier-Lavigne, M. (2004). PTK7/CCK-4 is a novel regulator of planar cell polarity in vertebrates. *Nature* **430**, 93-98.
Lu, F. I., Thisse, C. and Thisse, B. (2011). Identification and mechanism of regulation of the zebrafish dorsal determinant. *Proc. Natl. Acad. Sci. USA* **108**, 15876-15880.
Lui, T. T., Lacroix, C., Ahmed, S. M., Goldenberg, S. J., Leach, C. A., Daulat, A. M. and Angers, S. (2011). The ubiquitin-specific protease USP34 regulates axin stability and Wnt/β-catenin signaling. *Mol. Cell. Biol.* **31**, 2053-2065.
Maeder, M. L., Thibodeau-Beganny, S., Osiak, A., Wright, D. A., Anthony, R. M., Eichtinger, M., Jiang, T., Foley, J. E., Winfrey, R. J., Townsend, J. A. et al. (2008). Rapid 'open-source' engineering of customized zinc-finger nucleases for highly efficient gene modification. *Mol. Cell* **31**, 294-301.
Martin, B. L. and Kimelman, D. (2008). Regulation of canonical Wnt signaling by Brachyury is essential for posterior mesoderm formation. *Dev. Cell* **15**, 121-133.
Martin, B. L. and Kimelman, D. (2012). Canonical Wnt signaling dynamically controls multiple stem cell fate decisions during vertebrate body formation. *Dev. Cell* **22**, 223-232.
Megason, S. G. and Fraser, S. E. (2003). Digitizing life at the level of the cell: high-performance laser-scanning microscopy and image analysis for in toto imaging of development. *Mech. Dev.* **120**, 1407-1420.
Meng, X., Noyes, M. B., Zhu, L. J., Lawson, N. D. and Wolfe, S. A. (2008). Targeted gene inactivation in zebrafish using engineered zinc-finger nucleases. *Nat. Biotechnol.* **26**, 695-701.
Mikels, A. J. and Nusse, R. (2006). Purified Wnt5a protein activates or inhibits beta-catenin-TCF signaling depending on receptor context. *PLoS Biol.* **4**, e115.

Miller, M. A. and Steele, R. E. (2000). Lemon encodes an unusual receptor protein-tyrosine kinase expressed during gametogenesis in Hydra. *Dev. Biol.* **224**, 286-298.
Moon, R. T., Campbell, R. M., Christian, J. L., McGrew, L. L., Shih, J. and Fraser, S. (1993). Xwnt-5A: a maternal Wnt that affects morphogenetic movements after overexpression in embryos of Xenopus laevis. *Development* **119**, 97-111.
Moon, R. T., Brown, J. D. and Torres, M. (1997). WNTs modulate cell fate and behavior during vertebrate development. *Trends Genet.* **13**, 157-162.
Mossie, K., Jallal, B., Alves, F., Sures, I., Plowman, G. D. and Ullrich, A. (1995). Colon carcinoma kinase-4 defines a new subclass of the receptor tyrosine kinase family. *Oncogene* **11**, 2179-2184.
Müller-Tidow, C., Schwäble, J., Steffen, B., Tidow, N., Brandt, B., Becker, K., Schulze-Bahr, E., Halfter, H., Vogt, U., Metzger, R. et al. (2004). High-throughput analysis of genome-wide receptor tyrosine kinase expression in human cancers identifies potential novel drug targets. *Clin. Cancer Res.* **10**, 1241-1249.
Nowotschin, S., Ferrer-Vaquer, A., Concepcion, D., Papaioannou, V. E. and Hadjantonakis, A. K. (2012). Interaction of Wnt3a, Msgn1 and Tbx6 in neural versus paraxial mesoderm lineage commitment and paraxial mesoderm differentiation in the mouse embryo. *Dev. Biol.* **367**, 1-14.
Park, M. and Moon, R. T. (2002). The planar cell-polarity gene stbm regulates cell behaviour and cell fate in vertebrate embryos. *Nat. Cell Biol.* **4**, 20-25.
Paudyal, A., Damrau, C., Patterson, V. L., Ermakov, A., Formstone, C., Lalanne, Z., Wells, S., Lu, X., Norris, D. P., Dean, C. H. et al. (2010). The novel mouse mutant, chuzhoi, has disruption of Ptk7 protein and exhibits defects in neural tube, heart and lung development and abnormal planar cell polarity in the ear. *BMC Dev. Biol.* **10**, 87.
Peradziryi, H., Kaplan, N. A., Podleschny, M., Liu, X., Wehner, P., Borchers, A. and Tolwinski, N. S. (2011). PTK7/Otk interacts with Wnts and inhibits canonical Wnt signalling. *EMBO J.* **30**, 3729-3740.
Polakis, P. (2007). The many ways of Wnt in cancer. *Curr. Opin. Genet. Dev.* **17**, 45-51.
Prebet, T., Lhoumeau, A. C., Arnoulet, C., Aulas, A., Marchetto, S., Audebert, S., Puppo, F., Chabannon, C., Sainty, D., Santoni, M. J. et al. (2010). The cell polarity PTK7 receptor acts as a modulator of the chemotherapeutic response in acute myeloid leukemia and impairs clinical outcome. *Blood* **116**, 2315-2323.
Puppo, F., Thomé, V., Lhoumeau, A. C., Cibois, M., Gangar, A., Lembo, F., Belotti, E., Marchetto, S., Lécine, P., Prébet, T. et al. (2011). Protein tyrosine kinase 7 has a conserved role in Wnt/β-catenin canonical signalling. *EMBO Rep.* **12**, 43-49.
Ramel, M. C. and Lekven, A. C. (2004). Repression of the vertebrate organizer by Wnt8 is mediated by Vent and Vox. *Development* **131**, 3991-4000.
Roszko, I., Sawada, A. and Solnica-Krezel, L. (2009). Regulation of convergence and extension movements during vertebrate gastrulation by the Wnt/PCP pathway. *Semin. Cell Dev. Biol.* **20**, 986-997.
Ryu, S. L., Fujii, R., Yamanaka, Y., Shimizu, T., Yabe, T., Hirata, T., Hibi, M. and Hirano, T. (2001). Regulation of dharma/bozozok by the Wnt pathway. *Dev. Biol.* **231**, 397-409.
Schier, A. F. and Talbot, W. S. (2005). Molecular genetics of axis formation in zebrafish. *Annu. Rev. Genet.* **39**, 561-613.
Shnitsar, I. and Borchers, A. (2008). PTK7 recruits dsh to regulate neural crest migration. *Development* **135**, 4015-4024.
Simons, M. and Mlodzik, M. (2008). Planar cell polarity signaling: from fly development to human disease. *Annu. Rev. Genet.* **42**, 517-540.
Solnica-Krezel, L. and Driever, W. (2001). The role of the homeodomain protein Bozozok in zebrafish axis formation. *Int. J. Dev. Biol.* **45**, 299-310.
Strutt, H. and Strutt, D. (2009). Asymmetric localisation of planar polarity proteins: Mechanisms and consequences. *Semin. Cell Dev. Biol.* **20**, 957-963.
Tamai, K., Semenov, M., Kato, Y., Spokony, R., Liu, C., Katsuyama, Y., Hess, F., Saint-Jeannet, J. P. and He, X. (2000). LDL-receptor-related proteins in Wnt signal transduction. *Nature* **407**, 530-535.
Topczewski, J., Sepich, D. S., Myers, D. C., Walker, C., Amores, A., Lele, Z., Hammerschmidt, M., Postlethwait, J. and Solnica-Krezel, L. (2001). The zebrafish glypican knypek controls cell polarity during gastrulation movements of convergent extension. *Dev. Cell* **1**, 251-264.
Ungar, A. R., Kelly, G. M. and Moon, R. T. (1995). Wnt4 affects morphogenesis when misexpressed in the zebrafish embryo. *Mech. Dev.* **52**, 153-164.
van Amerongen, R., Mikels, A. and Nusse, R. (2008). Alternative wnt signaling is initiated by distinct receptors. *Sci. Signal.* **1**, re9.
van de Water, S., van de Wetering, M., Joore, J., Esseling, J., Bink, R., Clevers, H. and Zivkovic, D. (2001). Ectopic Wnt signal determines the eyeless phenotype of zebrafish masterblind mutant. *Development* **128**, 3877-3888.
van der Geer, P., Hunter, T. and Lindberg, R. A. (1994). Receptor protein-tyrosine kinases and their signal transduction pathways. *Annu. Rev. Cell Biol.* **10**, 251-337.
Veeman, M. T., Slusarski, D. C., Kaykas, A., Louie, S. H. and Moon, R. T. (2003). Zebrafish prickle, a modulator of noncanonical Wnt/Fz signaling, regulates gastrulation movements. *Curr. Biol.* **13**, 680-685.
Wallingford, J. B. and Harland, R. M. (2002). Neural tube closure requires Dishevelled-dependent convergent extension of the midline. *Development* **129**, 5815-5825.
Wang, Y. (2009). Wnt/Planar cell polarity signaling: a new paradigm for cancer therapy. *Mol. Cancer Ther.* **8**, 2103-2109.
Wehner, P., Shnitsar, I., Urlaub, H. and Borchers, A. (2011). RACK1 is a novel interaction partner of PTK7 that is required for neural tube closure. *Development* **138**, 1321-1327.
Westerfield, M. (2007). *The Zebrafish Book: a Guide for the Laboratory Use of Zebrafish (Danio Rerio)*. Eugene, OR: University of Oregon Press.
Winberg, M. L., Tamagnone, L., Bai, J., Comoglio, P. M., Montell, D. and Goodman, C. S. (2001). The transmembrane protein Off-track associates with Plexins and functions downstream of Semaphorin signaling during axon guidance. *Neuron* **32**, 53-62.
Wodarz, A. and Nusse, R. (1998). Mechanisms of Wnt signaling in development. *Annu. Rev. Cell Dev. Biol.* **14**, 59-88.
Wylie, C., Kofron, M., Payne, C., Anderson, R., Hosobuchi, M., Joseph, E. and Heasman, J. (1996). Maternal beta-catenin establishes a 'dorsal signal' in early Xenopus embryos. *Development* **122**, 2987-2996.
Xie, X. W., Liu, J. X., Hu, B. and Xiao, W. (2011). Zebrafish foxo3b negatively regulates canonical Wnt signaling to affect early embryogenesis. *PLoS ONE* **6**, e24469.
Yamaguchi, T. P., Bradley, A., McMahon, A. P. and Jones, S. (1999a). A Wnt5a pathway underlies outgrowth of multiple structures in the vertebrate embryo. *Development* **126**, 1211-1223.
Yamaguchi, T. P., Takada, S., Yoshikawa, Y., Wu, N. and McMahon, A. P. (1999b). T (Brachyury) is a direct target of Wnt3a during paraxial mesoderm specification. *Genes Dev.* **13**, 3185-3190.
Yen, W. W., Williams, M., Periasamy, A., Conaway, M., Burdsal, C., Keller, R., Lu, X. and Sutherland, A. (2009). PTK7 is essential for polarized cell motility and convergent extension during mouse gastrulation. *Development* **136**, 2039-2048.
Yin, C., Kiskowski, M., Pouille, P. A., Farge, E. and Solnica-Krezel, L. (2008). Cooperation of polarized cell intercalations drives convergence and extension of presomitic mesoderm during zebrafish gastrulation. *J. Cell Biol.* **180**, 221-232.
Yin, C., Ciruna, B. and Solnica-Krezel, L. (2009). Convergence and extension movements during vertebrate gastrulation. *Curr. Top. Dev. Biol.* **89**, 163-192.
Zallen, J. A. (2007). Planar polarity and tissue morphogenesis. *Cell* **129**, 1051-1063.

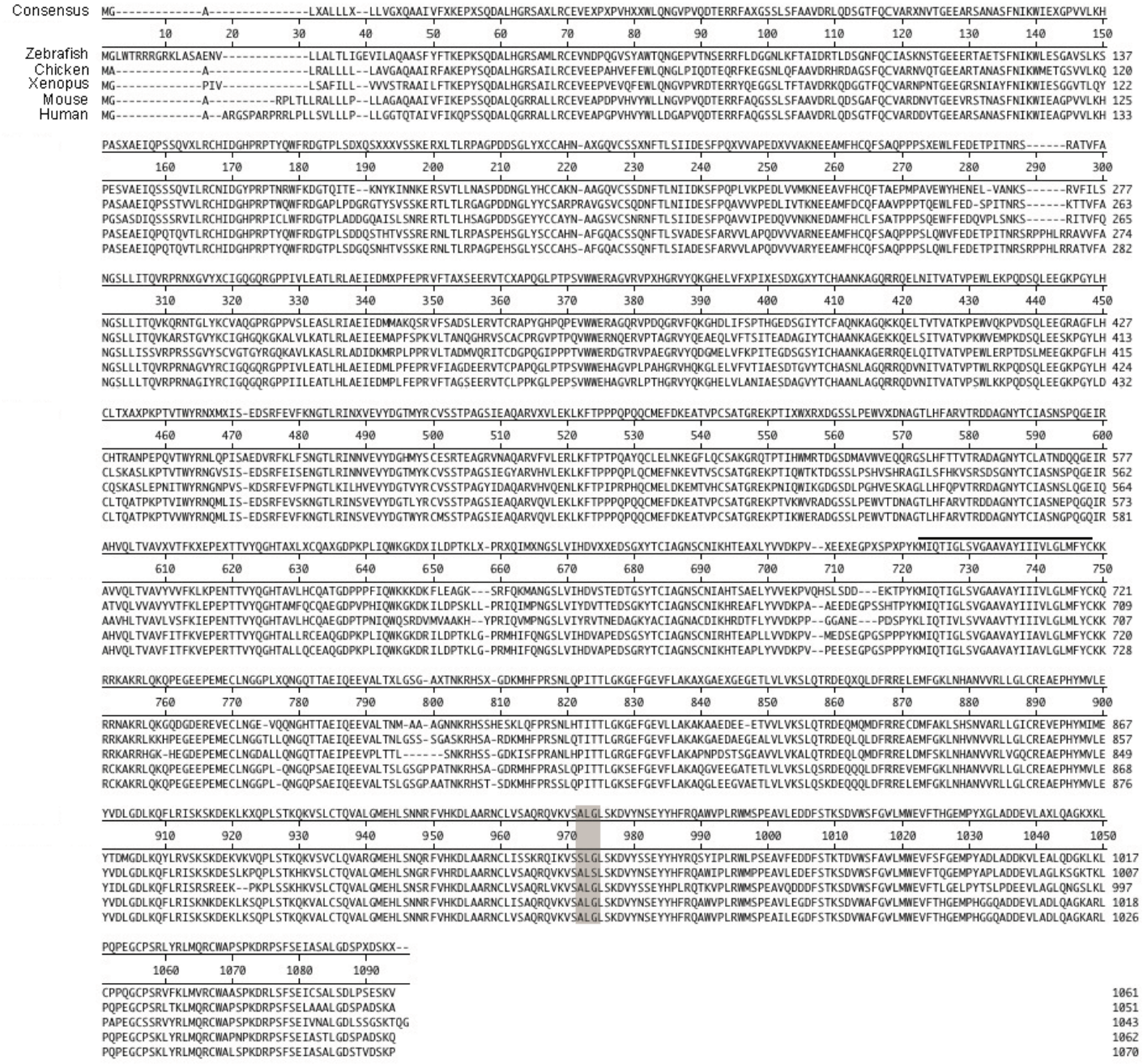

Fig. S1. Ptk7 protein sequence. Predicted amino acid sequence of zebrafish Ptk7 protein aligned with chicken, *Xenopus*, mouse and human orthologues. The predicted transmembrane domain is indicated by a single line. The modified 'DFG' triplet is indicated by the shaded box.

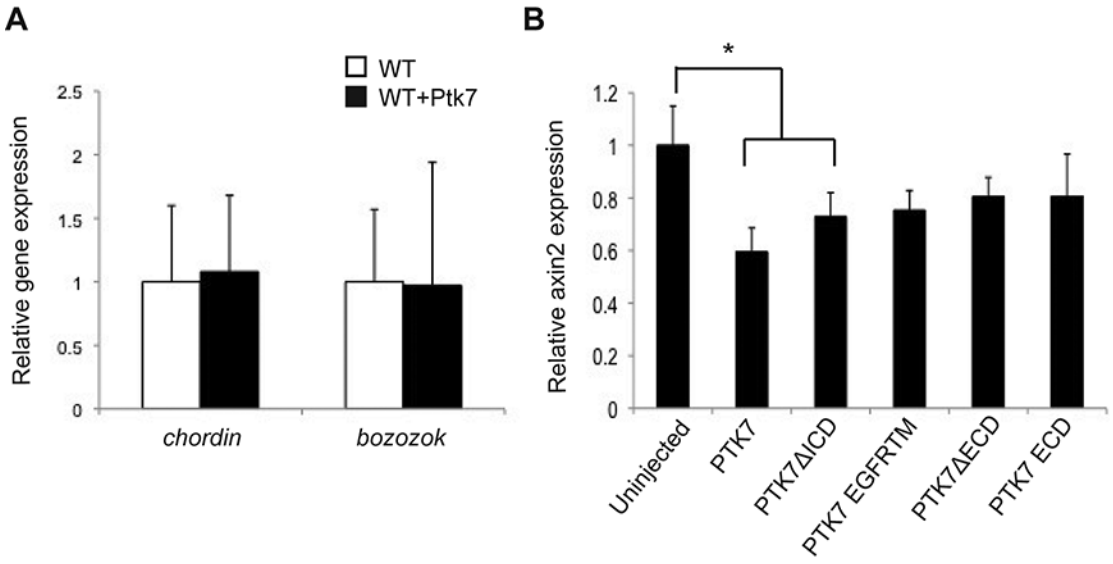

Fig. S2. Plasma membrane-tethered Ptk7 extracellular domain can inhibit endogenous ventral Wnt/β-catenin target gene expression. (**A**) qRT-PCR to detect relative *chd* (*P*=0.87) and *boz* (*P*=0.95) expression levels at 4 hpf in wild-type (WT) embryos and embryos injected with *ptk7* (400 pg) mRNA within 10 minutes of fertilisation. (**B**) qRT-PCR to detect relative *axin2* expression levels at shield stage in wild-type embryos, and embryos injected with: *ptk7* (400 pg), *ptk7ΔICD* (300 pg), *ptk7 egfrTM* (400 pg), *ptk7ΔECD* (300 pg) or *ptk7 ECD* (300 pg) mRNA. Error bars represent the standard error of the fold change. Each graph is representative of two independent experiments with three technical replicates each.**P*<0.05, Student's *t*-test.

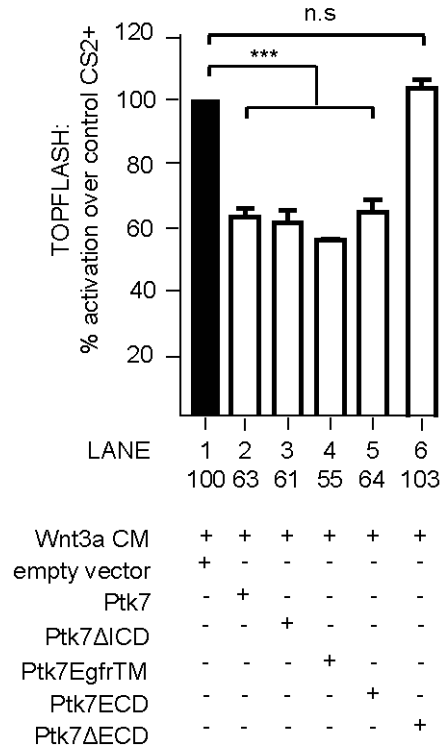

Fig. S3. Ptk7 inhibits Wnt3a-induced luciferase activity in HEK293T cells. To activate Wnt/β-catenin signaling Wnt3a-conditioned medium (Wnt3a CM) was used. Cells were transfected with empty vector, *ptk7*, *ptk7ΔICD*, *ptk7egfrTM*, *ptk7ΔECD* and *ptk7 ECD* expression plasmids. The graph represents TOPFLASH luciferase activity in three independent experiments. The luciferase activity of Wnt3a-treated empty vector (CS2+)-transfected cells was set to 1. Error bars represent s.e.m. ****P*<0.001, Student's *t*-test. n.s., not significant.

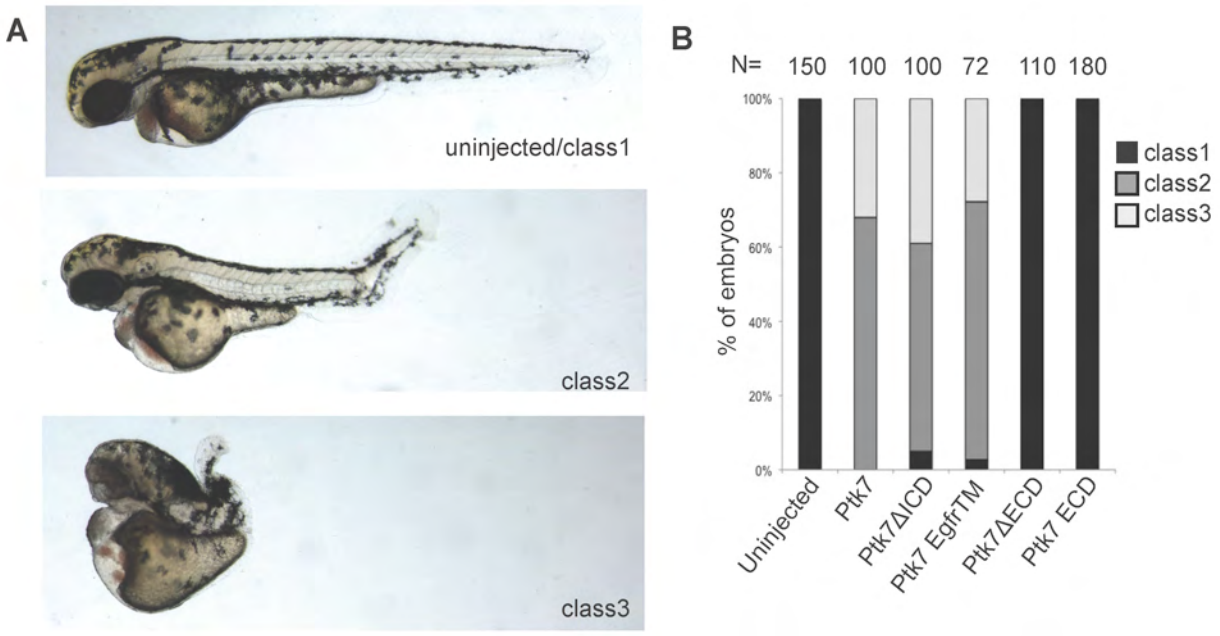

Fig S4. Plasma membrane-tethered extracellular domain is required for Ptk7 overexpression activity. (**A**) Class of phenotypes induced by *ptk7* overexpression: wild-type/class 1; class 2, axial extension defects as well as dorsal curvatures of the posterior tail; class 3, mild to severe dorsalisation. (**B**) Distribution of phenotypes in embryos injected with *ptk7* (400 pg), *ptk7ΔICD* (300 pg), *ptk7 egfrTM* (400 pg), *ptk7ΔECD* (300 pg) and *ptk7 ECD* (300 pg) mRNA.

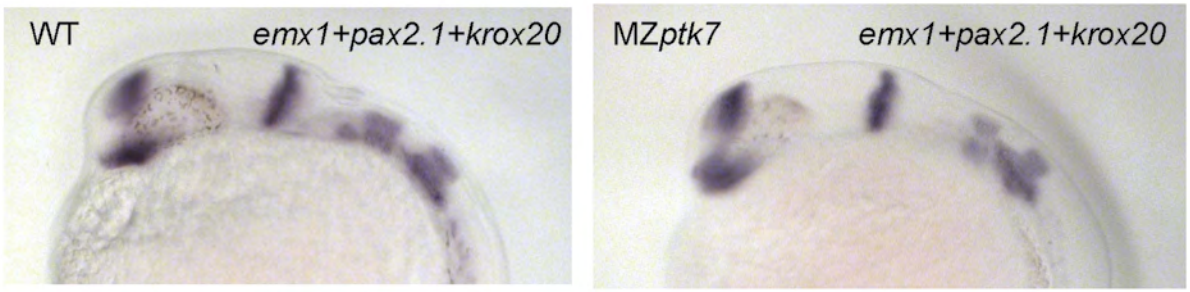

Fig. S5. MZ*ptk7*^{hsc9} embryos do not display CNS dorsoventral patterning defects. Whole-mount *in situ* hybridization of wild-type (WT) and MZ*ptk7* embryos at 24 hpf stained for *emx1*, *pax2.1* and *krox20* to mark the forebrain, midbrain-hindbrain boundary and posterior rhombomeres, respectively.

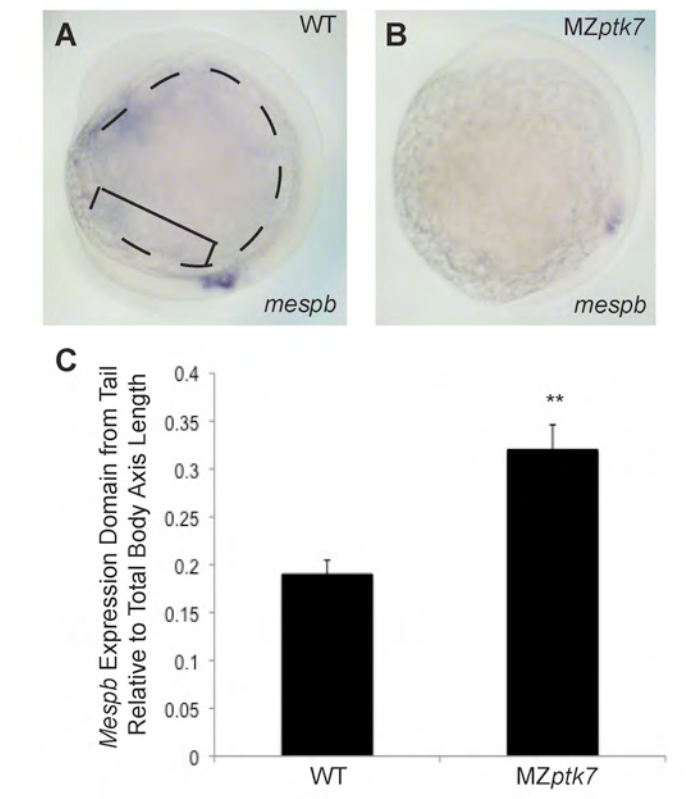

Fig. S6. MZ*ptk7*^{hsc9} mutants display tailbud patterning defects. (**A**,**B**) Whole-mount *in situ* hybridization of *mespb* expression, which delineates the anterior extent of pre-somitic mesoderm in wild-type (A) and MZ*ptk7*^{hsc9} mutant (B) embryos. *Mespb* expression is shifted anterior relative to total body axis length in MZ*ptk7*^{hsc9}. (**C**) Quantification of the ratio of the distance between the most posterior part of the embryonic tail (bracket in A) and the most posterior extent of the *mespb* expression domain to the total body axis length (dashed line in A) from head to tail in wild-type (WT) and MZ*ptk7*^{hsc9} at the 10- to 12-somite stage. Student's *t*-test, ***P*=0.0016. Error bars represent s.d.

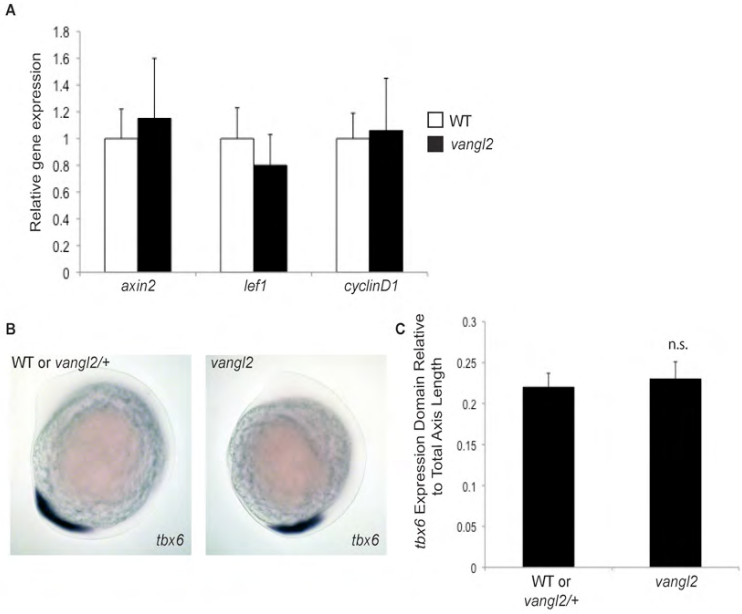

Fig. S7. Abnormal PCP does not disrupt Wnt/β-catenin signaling or posterior tissue fate specification. (**A**) qRT-PCR to analyze expression of Wnt/β-catenin target genes in *vangl2* mutants relative to wild-type (WT) reveals no difference in expression levels of *axin2* (*P*=0.6314, Student's *t*-test), *lef1* (*P*=0.3469, Student's *t*-test), or *cyclin D1* (*P*=0.8825, Student's *t*-test). Error bars represent standard error of the fold change. Each graph is representative of two independent experiments with three technical replicates each. (**B**) Lateral views of whole-mount *in situ* hybridization for the posterior mesodermal marker *tbx6* in wild-type/*vangl2*$^{+/-}$ and *vangl2* mutant embryos. (**C**) Quantification of the size of the *tbx6* expression domain relative to the total embryonic body length in WT and *vangl2* mutant embryos. The *tbx6* expression domain is not significantly expanded in *vangl2* mutant embryos. n.s., not significant, Students *t*-test.

Table S1. The sequences for left (L) and right (R) zinc-fingers used for generation of the *ptk7* mutant

	Sequence (5′-3′)
L1	ggtacccgccccttccagtgtcgcatttgcatgcggaacttttcgaccacccacaaccttatgaggcatacccgtactcataccggwgaaaaaccgtttc agtgtcggatmtgtatgcgaaatttctccgagagcacgaccttgatcaggcatctacgtacgcacaccggcgagaagccattccaatgccgaatatgca tgcgcaacttcagtgtggcggggaacctgcggcggcacctaaaaacccacctgaggggatcc
L2	ggtacccgccccttccagtgtcgcatttgcatgcggaacttttcgacccccccacaaccttctgaggcatacccgtactcataccggtgaaaaaccgtttca gtgtcggatctgtatgcgaaatttctccgaccccagcgtcttgacgcgccatctacgtacgcacaccggcgagaagccattccaatgccgaatatgcatg cgcaacttcagtctgagcaccaacctgacgaggcacctaaaaacccacctgaggggatcc
R1	ggtacccgccccttccagtgtcgcatttgcatgcggaacttttcgaagcacagcaaccttacgcggcatacccgtactcataccggtgaaaaaccgtttc agtgtcggatctgtatgcgaaatttctcccggcgggccatcttggccaaccatctacgtacgcacaccggcgagaagccattccaatgccgaatatgcat gcgcaacttcagtcagagcgtcaacctgcggcggcacctaaaaacccacctgaggggatcc
R2	ggtacccgccccttccagtgtcgcatttgcatgcggaacttttcgaggcagaccaaccttatccgccatacccgtactcataccggtgaaaaaccgtttca gtgtcggatctgtatgcgaaatttctcccgcaacgaggtgttgatgaaccatctacgtacgcacaccggcgagaagccattccaatgccgaatatgcatg cgcaacttcagtcagcaggtgaacctggtgcgccacctaaaaacccacctgaggggatcc

Table S2. Cloning and quantitative RT-PCR primer sets

	Primer pair(s)
ptk7	forward 5'-ATGGGCTTATGGACGAGAAGACG-3' reverse 5'-TCAGACTTTGCTCTCGGAGGGCAG-3'
ptk7ΔICD	forward 5'-ATGGGCTTATGGACGAGAAGACG-3' reverse 5'-GTTGCTTCGAGGGAATTGTAG-3'
ptk7 egfrTM	forward1 5'-ATGGGCTTATGGACGAGAAGACG-3', reverse1 5'- GTCCTGCCCCTTCTGGAGCCTCTTGGCGTTGCGTCTCTGCTTCAGAACGG CCACTCCAAGAGCCAGAATAACAAACGCCAGTAGACCTCCG-3' forward2 5'-AGAGACGCAACGCCAAGAG-3' reverse2 5'-GTTGCTTCGAGGGAATTGTAG-3'
ptk7ΔECD	forward1 5'-ATGGGGGTTGGGAGGAGTTAG-3' reverse1 5'- TCTCATCGTCTGATAAGGAGTGCTGCACTGGTTTTTCTGAGAGACACAC AGATGGGTCTG-3' forward2 5'-GAAAAACCAGTGCAGCACTCCTTATCAG-3' reverse2 5'-TCAGACTTTGCTCTCGGAGGGCAG-3'
ptk7 ECD	forward 5'-ATGGGCTTATGGACGAGAAGACG-3' reverse 5'-ATAAGGGGTCTTCTCATCGTCTG-3'
axin2	forward 5'-ACCAAGCACAAGCCCCACAGC-3' reverse 5'-ATGCCCACTGCTTCCGCCAC-3'
cyclin D1	forward 5'-CTGCGCAAACACGCCCAGAC-3' reverse 5'-TACCGCTGCAGCAACACTGCC-3'
lef1	forward 5'-AGGCCACCCGTACCCGAGTT-3' reverse 5'-GGGAGGCGAGAGAGAGCCGT-3'
ptk7	forward 5'-CTCAGCCGCTGGTGAAGCCTG-3' reverse 5'-AACAGCGGGCATCGGCTCG-3'
bozozok	forward 5'-CACGGGCCTCAGCGAGGAGA-3' reverse 5'-AGCGTGTTTGTCAGCGCAGGT-3'
chordin	forward 5'-GCATCCTTTCGTCCCGCCGT-3' reverse 5'-GGCGGGCACGTCACCTTCTC-3'
goosecoid	forward 5'-CAGGACCTCCAGCGCCGAAC-3' reverse 5'-TCGGCCCCTGGACGTGAAGT-3'
vox	forward 5'-GCGCGCGGATTTTCTGCTGC-3' reverse 5'-GGGAACGGGAGCCGCTGTCT-3'
gapdh	forward 5'-GGGCTGCCAAGGCTGTAGGC-3' reverse 5'-TGGGGGTGGGGACACGGAAG-3'
ef1alpha	forward 5'-GCCATCTGATCTACAAATGCGGTG-3' reverse 5'-TTTGCTGGTCTCGAATTTCCAAAGG-3'